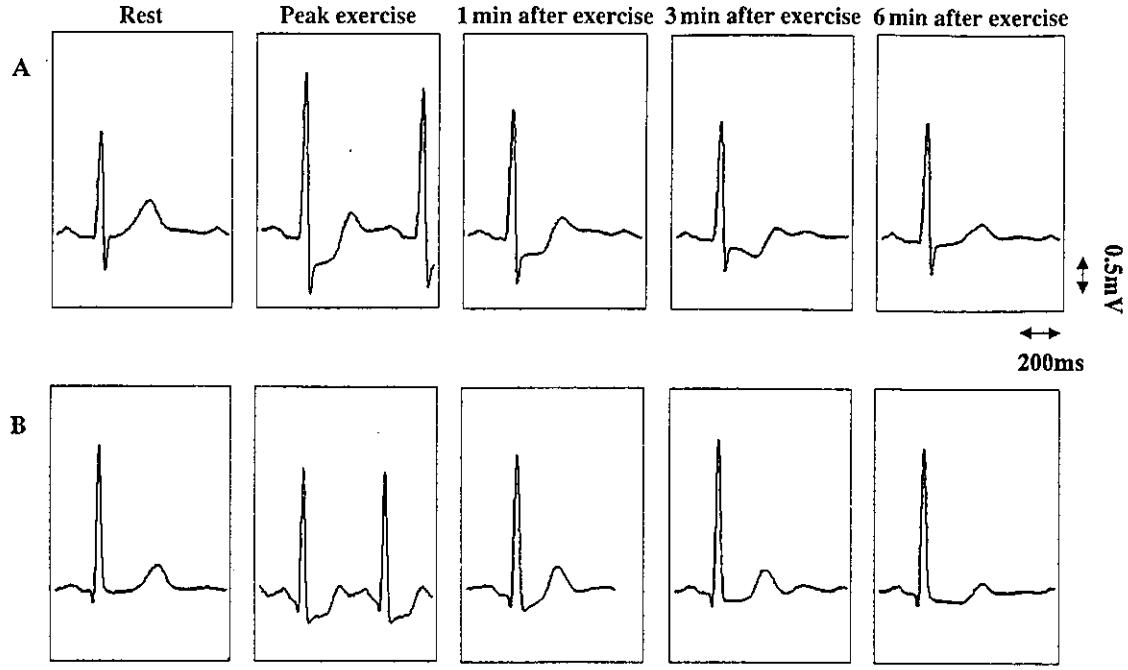

Fig 1. Representative exercise ECG from a patient with (A) true-positive (TP: V_5) and (B) false-positive (FP: V_6) ST-segment response. In the patient with a TP response, slow-rising ST-segment depression at peak exercise and at 1 min after exercise became downsloping at 3 min followed by its recovery at 6 min. That is, the ST slope transiently decreased soon after exercise but increased with time in late recovery. In the subject with a FP response, a horizontal ST-segment depression at postexercise 3 min became downsloping at 6 min; that is, the ST slope decreased in this late recovery.

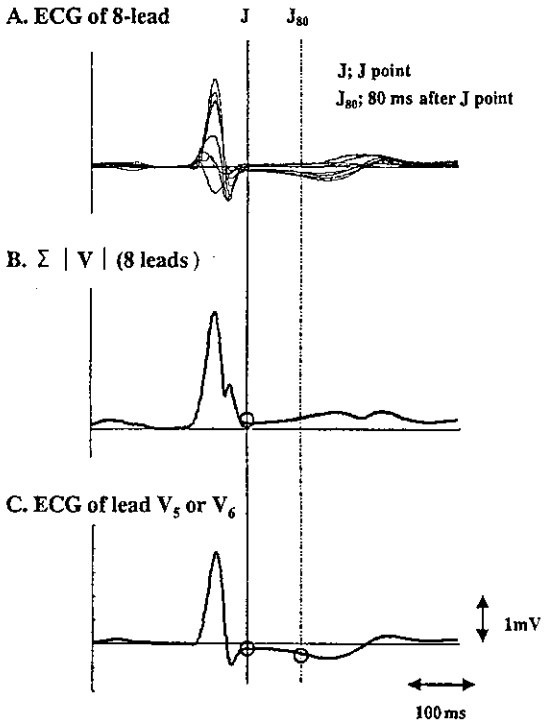

Fig 2. Computer measurements of the ST slope. From ECG data for all 8 leads (A), we computed the algebraic sum ($\Sigma|V|$) of the absolute value of voltage relative to the isoelectric Q-Q baseline (B), which was used to determine the J-point. Once the J-point was determined, ST-segment displacements from the isoelectric Q-Q baseline at the J-point and at J_{80} were measured automatically (C). The ST slope is derived as the slope connecting these 2 points. Vertical solid and broken lines indicate the J-point and J_{80}, respectively.

malities such as prior myocardial infarction, ST-segment depression, T-wave inversion, LVH, or bundle branch block. We also excluded patients with atrial fibrillation or frequent extrasystole (>10 beats/min) and those with exercise-induced ST-segment elevation (≥0.1 mV). All subjects gave informed consent.

Patients were divided into the 2 groups according to the results of coronary angiography and exercise SPECT performed within 3 months after treadmill testing. The TP group comprised 134 patients (62±9 years) who had angiographical coronary artery stenosis (>50% luminal narrowing). Inducible ischemia was confirmed by the presence of reversible defects corresponding to coronary lesions. The FP group included 64 subjects (63±10 years) with normal exercise SPECT images. Of them, 19 (30%) had undergone coronary angiography and none had significant CAD.

We investigated the presence of a history of hypertension, which may be associated with a high incidence of FPD in patients with mild LVH only discernible by echocardiographic study[9,10]

Treadmill Exercise ECG

Exercise testing was performed according to our protocol, which was similar to the modified Bruce protocol[11] We performed the test using a treadmill system (Formula, Esaote, Italy), while simultaneously digitizing the ECG data at 500 Hz (12-bit resolution) from rest, during exercise, and into recovery for at least 6 min. A hard copy of the standard 12-lead ECG at a paper speed of 25 mm/s at rest, at the end of each stage, at peak exercise, and every minute into recovery was produced. Termination of exercise was decided by the occurrence of exhaustion, ST-segment depression >0.3 mV, significant arrhythmias, moderately severe angina, inadequate blood pressure response, or the attainment of 90% predicted maximal heart rate.

Table 1 Clinical Characteristics of the Study Population

	FP (n=64)	TP (n=134)
M/F (n, %)	34/30 (53/47)	118/16 (88/12)**
Age (years)	63±10	62±9
Coronary risk factors		
Hypertension (%)	44	60*
Diabetes mellitus (%)	14	40*
Medications		
Nitrates (%)	11	60**
β-blockers (%)	16	57**
Calcium-antagonists (%)	27	68**
Coronary artery disease		
LMT (%)	–	1
SVD (%)	–	46
DVD (%)	–	33
TVD (%)	–	20

*Values are mean±SD or numbers (percentage). **p<0.01 vs FP group. *p<0.05 vs FP group. FP, fales-positive; TP, true-positive; LMT, left main trunk disease; SVD, single vessel disease; DVD, double vessel disease; TVD, triple vessel disease.*

On the ECG hard copies, we identified a significant ST-segment depression according to the following criteria: (1) horizontal or downsloping ST-segment displacement at the J-point ≥0.1 mV; and (2) upsloping ST-segment displacement at J80 ≥0.15 mV in at least 3 consecutive beats at peak exercise. Arterial blood pressure was measured by a sphygmomanometer at the end of each stage, peak exercise and recovery.

ECG Analysis

For the standard 12-lead ECG, only 2 of 6 limb leads are actually recorded, and the other 4 leads are derived mathematically from these 2 leads[12] Our stress system capable of reproducing the 12-lead ECG actually records 2 unique limb leads (leads I and II) and 6 precordial leads in a similar manner. We performed the following analysis using the digitized ECG data set of 8 leads (I, II, and V_{1-6}; Fig 2A).

To determine the ST slope, we found the peak of each R wave in lead V_5, with which the QRS-T complex was averaged over 5 beats to improve the signal-to-noise ratio. On the QRS-T complex, we measured ST-segment displacement at peak exercise and at every minute during the first 6 min postexercise, in a lead with a greater ST-segment depression at peak exercise of either lead V_5 or V_6. Because the J-point determination is occasionally difficult, we derived the algebraic sum ($\Sigma|V|$) of the absolute value of voltage relative to the isoelectric Q-Q baseline from all 8 leads (Fig 2B). With reference to this curve, we determined the J-point by detecting the point at which the curve most closely approached the baseline (the lowest point of the trough). If the curve did not have a distinct trough, the J-point was assumed to be the inflection point at which a steep descent of the curve was terminated. Once the J-point was determined, ST-segment displacement from the Q-Q baseline at the J-point and J80 was measured automatically (Fig 2C). From these 2 values, we calculated the ST slope (mV/s). The ST slope, treated as a continuous variable ranging from negative to positive values, was used for the later intra- and intergroup comparisons. The time-courses of ST-segment depression and ST slope from peak exercise to the 6-min recovery (every minute, 7 time points) were assessed.

Table 2 Exercise Test Results

	FP (n=64)	TP (n=134)	p value
Rest HR (beats/min)	72±11	67±11	<0.01
Rest SBP (mmHg)	139±22	132±19	<0.05
Peak HR (beats/min)	149±19	127±21	<0.01
Peak SBP (mmHg)	178±27	160±24	<0.01
Exercise time (s)	526±150	480±136	<0.05
Exercise-induced chest pain (%)	9	46	<0.01
ST-segment depression (mV)	–0.20±0.11	–0.22±0.12	<0.01

FP, fales-positive; TP, true-positive; HR, heart rate; SBP, systolic blood pressure.

Exercise Thallium-201 Scintigraphy

All subjects underwent bicycle exercise testing according to the same end points as defined earlier. At near-maximal exercise, thallium-201 was intravenously injected and the patient was encouraged to exercise for another 1 min. SPECT images were obtained at 15 min (initial images) and 4 h (delayed images). The images were reconstructed into transaxial tomograms, which were assessed by 2 experienced physicians unaware of the coronary anatomy. Thallium uptake in myocardial segments was classified as normal, mildly, moderately or severely reduced, or absent. A reversible defect was defined when the classification of uptake improved by at least one category from the initial to the delayed image.

Statistical Analysis

All data are presented as mean±SD. Unpaired t-test was used for comparisons between 2 groups. Differences in categorical variables were analyzed by chi-square analysis. The time-course of ST-segment depression and the ST slope were compared by analysis of variance for repeated measurement. When this test was significant, the Newman-Keuls post-hoc multiple comparison was performed.

For convenience in presentation, the term 'sensitivity' is used to measure the percentage of subjects who met the criteria for identifying FP results in the FP group. The term 'specificity' is used to measure the percentage of subjects who did not fulfill the criteria in the TP group.

Performance of diagnostic criteria was evaluated using receiver operating characteristic (ROC) curve analysis[13,14] The area under the curve (AUC), which is a measure of the discriminatory power of the index, was calculated for each variable and these areas were compared statistically[15] A p-value <0.05 was considered significant.

Results

Patient Characteristics

Although age was similar between the groups, the FP group included more females than the TP group (p<0.01, Table 1). Hypertension, common to both groups, was found more frequently in the TP (60%) group than in the FP group (44%, p<0.05). Approximately half of the TP patients (46%) had single-vessel disease.

Treadmill Exercise Test

Resting heart rate and systolic blood pressure were higher in the FP group than in the TP group (p<0.01 and p<0.05, respectively; Table 2). Exercise time, peak heart rate and peak systolic blood pressure were also higher in the FP group (p<0.05, p<0.01, and p<0.01, respectively). Chest

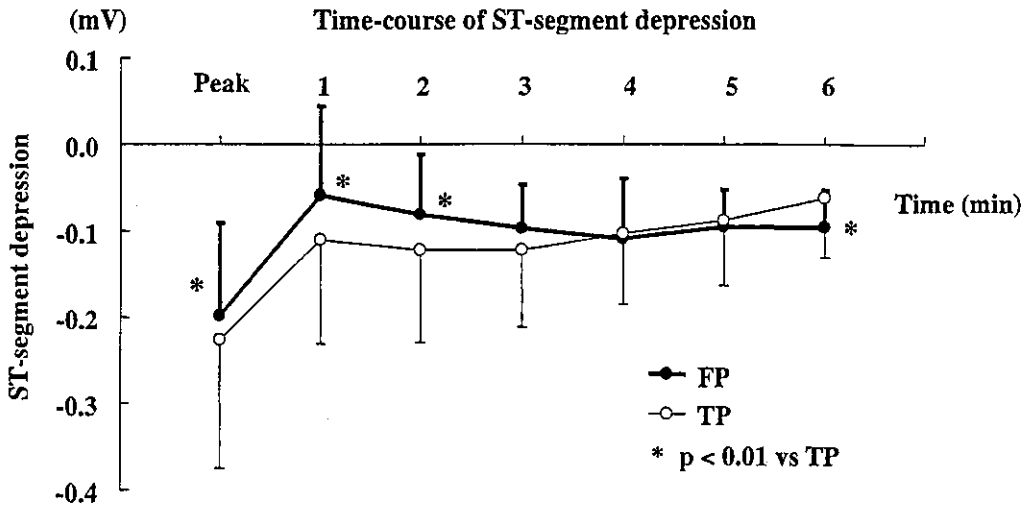

Fig 3. Comparison of the recovery time-course of ST-segment depression changes at the J80 between the false-positive (FP: closed circle) and true-positive (TP: open circle) groups. *p<0.01 vs TP.

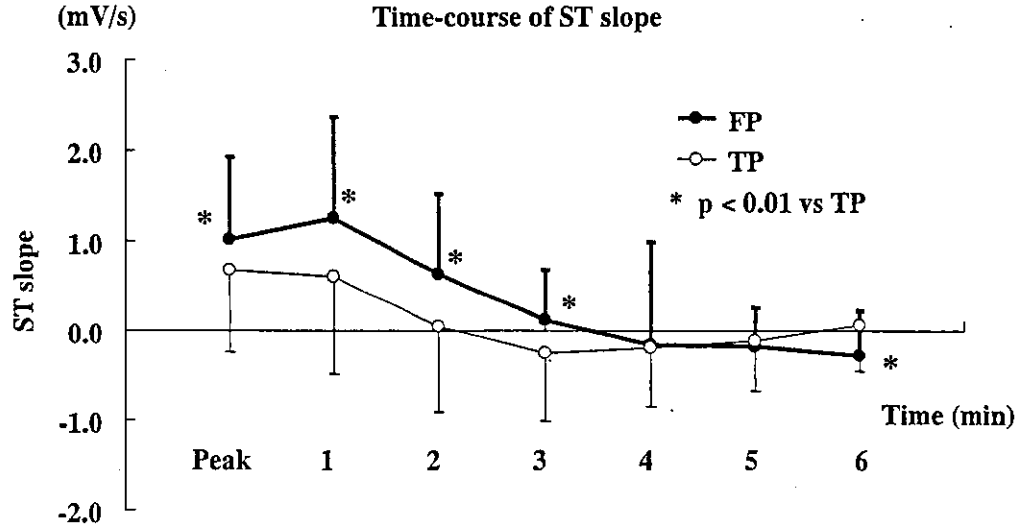

Fig 4. Comparison of the recovery time-course of changes in the ST slope between the false-positive (FP: closed circle) and true-positive (TP: open circle) groups. *p<0.01 vs TP.

pain, including atypical, equivocal, or typical features for angina, occurred in 46% of the TP group and 9% of the FP group (p<0.01) during the test. Maximal ST-segment depression (J80) was marginally but significantly greater in the TP (–0.23±0.15 mV) than in the FP group (–0.20± 0.11 mV, p=0.002, unpaired t-test).

Time-Course of ST-Segment Depression

Fig 3 shows the time-course of the recovery of ST-segment depression (J80). At peak exercise and in early recovery (at 1 and 2 min), ST-segment depression was significantly greater in the TP group (p<0.01, all) than in the FP group. No difference was observed at 3, 4, and 5 min. In the late recovery, ST-segment depression gradually recovered toward the baseline in the TP group, but remained unchanged in the FP group. Consequently, it was greater in the FP group than in the TP group at 6 min postexercise (p<0.01). Despite these differences, ST-segment depression at any time point hardly differed between the 2 groups because of a considerable overlap, evidenced by the large standard deviation.

Time-Course of the ST Slope

Fig 4 shows the time-course of the recovery of the ST slope. It decreased with time up to 3 min postexercise in each group. During this period, the ST slope was significantly lower in the TP group than in the FP group (all p<0.01). Thereafter it continued to decrease in the FP group, whereas it gradually recovered toward the baseline in the TP group. Thus, in the late recovery, the ST slope in the FP group changed in the opposite direction to that in the TP group.

Fig 5 shows the changes in the ST slope for each subject. In the FP group, the ST slope decreased between 3 and 6 min (0.12±0.55 to –0.28±0.50 mV/s, p<0.001), whereas it increased in the TP group (–0.25±0.77 to 0.06±0.52 mV/s, p<0.001). Most FP subjects (56/64, 88%) showed a decrease during this period, which was observed in only 19% of TP patients (25/134).

The time-course difference in the ST slope (ΔST Slope,

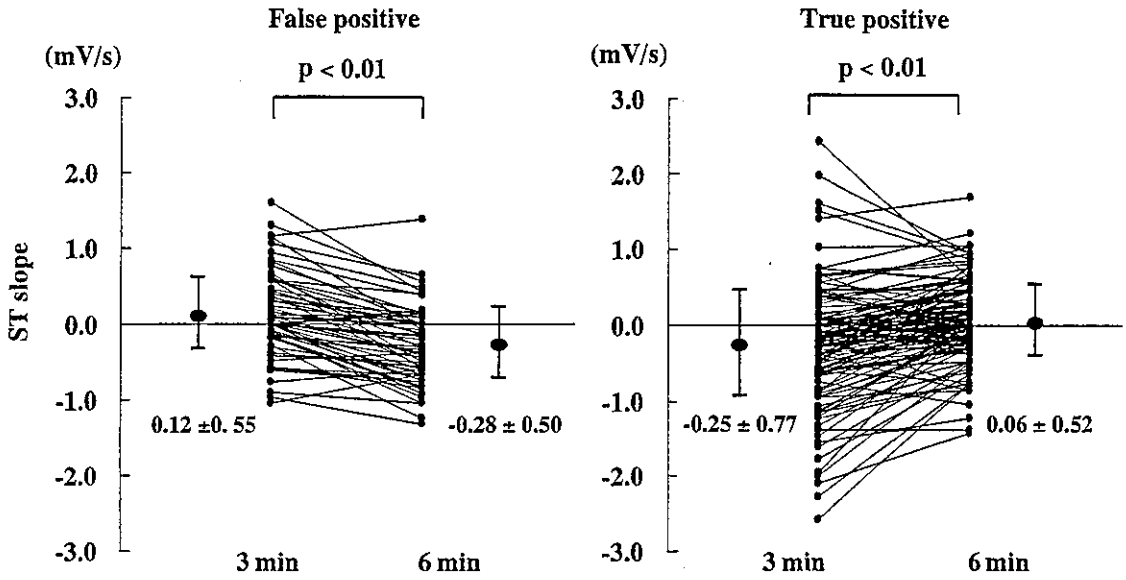

Fig 5. Changes in ST slope from 3 to 6 min after exercise in the false-positive (FP: Left) and true-positive (TP: Right) groups. Large closed circles and vertical lines represent means and 1 SD, respectively.

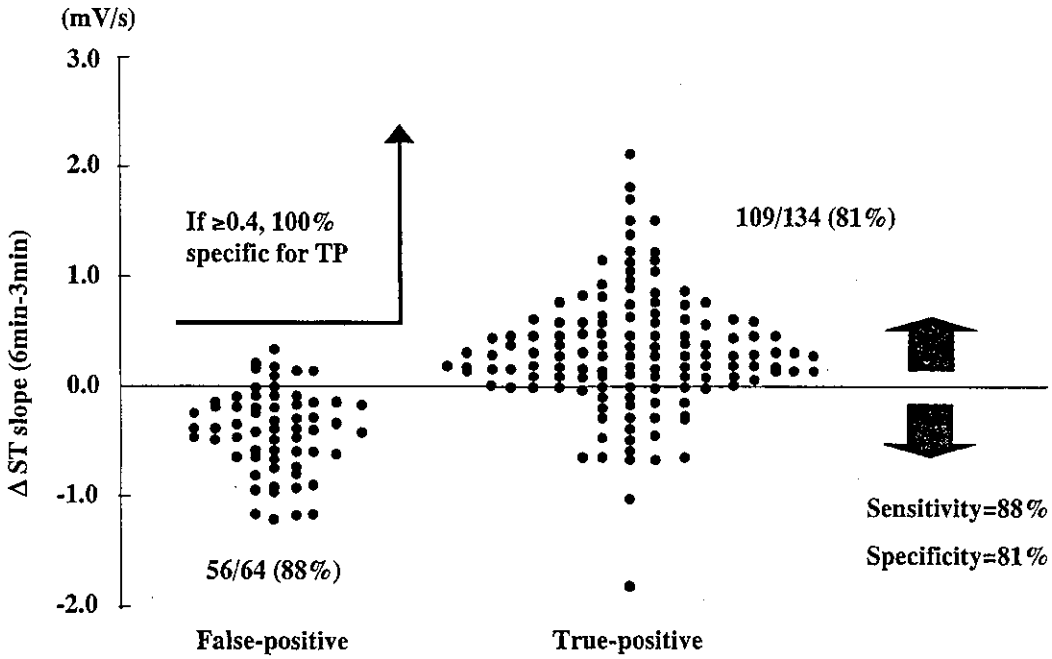

Fig 6. ΔST slope (ST slope at 6 min minus that at 3 min) is plotted for each subject in the false-positive (FP: Left) and true-positive (TP: Right) groups.

ST slope at 6 min minus that at 3 min) is plotted for each subject in Fig 6. When a decrease in the ST slope (ΔST Slope <0 mV/s) was set as the criterion for FPD, we could discriminate FP from TP patients with a sensitivity of 88% and a specificity of 81%. Conversely, its increase was highly predictive for TP patients; ΔST slope ≥0.4 mV/s was 100% predictive for TP patients (FP n=0, TP n=49) and ΔST slope ≥0.0 mV/s was 93% predictive for TP patients (FP n=8, TP n=109).

Because coronary angiography was not performed in 70% of the FP group, we performed separate subgroup analysis of subjects with (n=19) and without (n=44) angiography. As a result, the ST slope significantly decreased from postexercise 3- to 6-min in each group ($p<0.001$, for both groups). ΔST slope was very similar between the 2 groups (–0.36±0.43 mV/s with vs –0.42±0.35 mV/s without angiography, NS).

Comparison of Test Performance by ROC

Fig 7 shows the ROC curves describing the ability for the discrimination using the ST slope for 1, 3 and 6 min after exercise and ΔST slope. The AUC for ΔST slope was significantly greater than that of the ST slope obtained at any of the 3 time points ($p<0.01$, all).

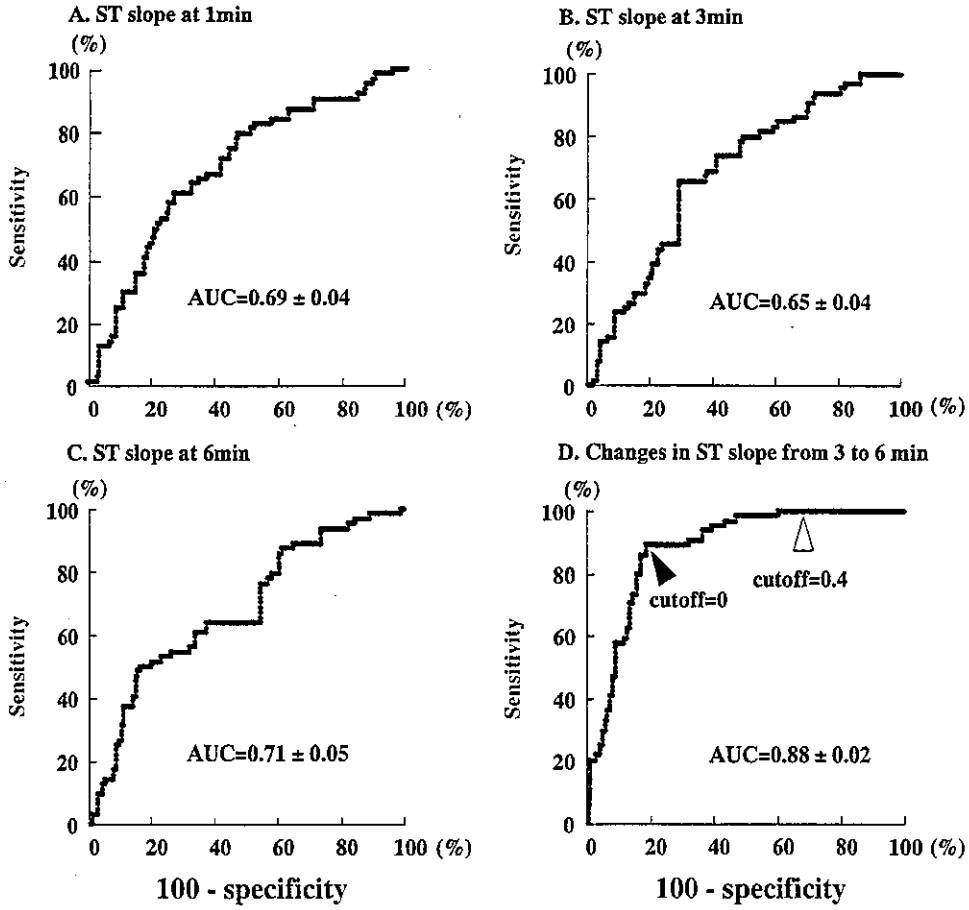

Fig 7. The receiver operating curve (ROC) for the ST slope at postexercise 1-min (A), 3-min (B) and 6-min (C), and for ΔST slope (D). The area under the ROC (AUC) for D was significantly greater than each AUC for A, B, or C ($p<0.001$, all). In (D), closed arrow indicates the diagnostic values (sensitivity 88%, specificity 81%) by using ΔST slope of <0.0 mV/s as the criterion for false-positive subjects. Open arrow indicates the values (sensitivity 37%, specificity 100%) by using ΔST slope of ≥0.4 mV/s as the criterion for true-positive patients.

Discussion

We have demonstrated that computer analysis of the recovery time-course of the ST slope is a simple, reliable method of discriminating FP from TP ST-segment responses. The accuracy using ΔST slope <0.0 mV/s as the criterion for FP response is considered to substantially improve the diagnostic value of exercise ECG. Furthermore, the finding that ΔST slope ≥0.4 mV/s could correctly identify TP responses without exception is important for the interpretation of the exercise ECG. One can consider that an exercise-induced ST-segment depression followed by an ST slope increase from post-exercise 3 to 6 min would credibly strengthen the diagnosis of CAD. To our best knowledge, there have been few studies conducted specifically to differentiate FP from TP ST-segment responses using a simple ECG marker in a relatively large population.

Diagnostic Value of ST Slope

To improve the accuracy of the exercise ECG, various indices have been proposed, including the degree of ST-segment depression[1,16,17] R wave amplitude changes[18,19] ST/HR slope[20,21] ST index[21,22] QT dispersion[2,23] ST slope[1,7,16,24,25] and concomitant changes in hemodynamic parameters[1,17] Each has been reported to improve accuracy; however, only a few are in clinical use, presumably because there has not been a dramatic increase in accuracy, the method is complicated or time-consuming, or both.

Downsloping or horizontal ST-segment depression is more specific for CAD than upsloping depression[1,7] Furthermore, the downsloping pattern has been reported as a marker for severe ischemia[26,27] Thus, the ST slope offers some useful diagnostic information. Also, in CAD patients, exercise-induced ST-segment depression often changes from an upsloping or horizontal pattern during exercise to a downsloping pattern in recovery[7,8] Therefore, because the ST-segment usually returns to baseline between 6 to 10 min postexercise, the ST-T time-course of CAD patients (ie, the TP response) can be characterized by a transient decrease in the ST slope soon after exercise with a gradual increase toward baseline in late recovery[7,8]

Unlike the characteristic time-course of the ST slope in CAD patients, individuals with FPD often show several patterns[5,8] one of which was observed in the present FP subjects. In it, the magnitude of ST-segment depression remained almost constant and the ST slope rather decreased from postexercise 3- to 6-min, whereas, in TP patients, both ST-segment depression and ST slope recovered toward baseline during this period. The directionally opposite ST slope changes emphasized the intergroup difference, contributing to accurate differentiation of the FPs from the TPs.

Different Recovery Time-Courses of the ST Slope in the TP and FP Groups

Despite the potential usefulness of ST-T time-course for diagnosis, few studies have focused on this possibility, especially in conjunction with the ST slope[5,8] In our analysis, the postexercise ST slope in TP patients progressively decreased up to 3 min, at which time it reached the lowest value of less than zero (downsloping) and gradually increased until 6 min. The mechanism(s) for this postexercise transient ST slope decrease in CAD is uncertain, but it could be, at least partially, explained by the effect of heart rate dependent J-point depression? In many CAD patients, tachycardia-induced J-point depression would lower the initial portion of ST-segment (ie, draw the ST-segment upward) during exercise, thereby obscuring or masking the downsloping depression, and the slowing of the heart rate following exercise would readily unmask the downsloping configuration. The subsequent progressive increase in ST slope from 3- to 6-min postexercise reflects the recovery process of the ischemia-induced electrophysiological impairment.

On the other hand, we observed a progressive decrease in the ST slope from 1- to 6-min postexercise in the FP subjects. After becoming negative at 4 min, the ST slope further decreased until 6 min, at which time the FP group eventually had a lower ST slope with a greater ST-segment depression than the TP group. This recovery time-course in FP subjects, characterized by the inappropriately late aggravation of ST-T abnormalities, has also been reported by Malcom et al who examined patients with mitral valve prolapse, a condition prone to FPD[5] The mechanism for this late aggravation is unknown. Although the FP group included many females (47%), in agreement with previous reports[1-3] it is noteworthy that the prevalence of hypertension was considerably high (44%) compared with that in the general population. In the presence of hypertension, implicated as one potential cause of FPD[9,10] strenuous exercise may acutely induce electrophysiological changes with late ST-segment aggravation by a mechanism such as the reduction of coronary flow reserve documented in those patients[6]

Advantages of Computer Analysis

Our computer analysis method using an 8-lead ECG ensures high-resolution analysis as well as objective and reproducible measurements; in particular, in terms of the J-point determination. Because it is difficult to precisely determine the J-point in a single lead with ST-segment depression, which may seriously affect the ST slope, we incorporated the QRS information of all 8 leads in a single complex (algebraic sum). Like other available systems, our stress system yields the ST slope in mV/s to one decimal place (eg, 0.3 mV/s). However, those values were not used for the analysis in the present study because the resolution was considered insufficient. More importantly, the measured values are occasionally inaccurate because of erroneous determination of the Q-Q baseline or J-point. Although ΔST slope could accurately differentiate FP from TP patients (Fig 6), the absolute values were very small in most subjects. We believe that high-resolution analysis can contribute to accurate diagnosis of the presence or absence of inducible ischemia by detecting the subtle ECG changes that are otherwise undetectable by conventional methods such as by a simple categorical judgement of the ST-segment shape[1,7]

Potential Limitations

First, FPD are frequently seen in patients with abnormal resting ECGs such as those with LVH[4,6] valvular disease[1,4,5] or cardiomyopathy[8] Because we examined subjects with a normal resting ECG, our findings cannot be extrapolated to those other categories of patients. Second, only patients with both angiographically and scintigraphically documented abnormalities were enrolled into the TP group because the diagnostic accuracy of SPECT is not perfect. This is probably the reason why the positive predictive value (68% = 134/198) for our entire population seems to be slightly lower than that previously reported. Furthermore, FPD was based on the normal exercise SPECT imaging, and 70% of FP subjects did not undergo angiography. Although the changes in ST slope from postexercise 3- to 6-min were similar in FP subjects with and without angiographic results, we cannot completely exclude the possibility that a number of FP subjects might have angiographical CAD.

Conclusion

Our study has demonstrated that a simple observation of the ST slope recovery time-course is very useful for discriminating FP from TP ST-segment depressions. Although our findings are currently confined to subjects with a normal resting ECG, they should enhance the diagnostic value of the exercise ECG and serve to reduce the number of more costly, time-consuming and invasive procedures.

Acknowledgments

This study was supported by a Research Grant for Cardiovascular Diseases (11C-7) from the Ministry of Health and Welfare of Japan, by a Grant-in-Aid for Scientific Research (C-11670730) from the Japan Society for the Promotion of Science, and by the Program for Promotion of Fundamental Studies in Health Science from the Organization for Pharmaceutical Safety and Research.

References

1. Pratt CM, Francis MJ, Divine GW, Young JB. Exercise testing in women with chest pain. *Chest* 1989; **95:** 139–144.
2. Stoletniy LN, Pai RG. Value of QT dispersion in the interpretation of exercise stress test in women. *Circulation* 1997; **96:** 904–910.
3. Alexander KP, Shaw LJ, Delong ER, Mark DB, Peterson ED. Value of exercise treadmill testing in women. *J Am Coll Cardiol* 1998; **32:** 1657–1664.
4. Bajaj R, Wasir HS. Value of analysis of the evolution of the pattern of the ST segment in exercise electrocardiogram. *Int J Cardiol* 1990; **29:** 323–326.
5. Malcom AD, Ahuja SP. The electrocardiographic response to exercise in 44 patients with mitral leaflet prolapse. *Eur J Cardiol* 1978; **8:** 359–370.
6. Marwick TH, Torelli J, Harjai K, Haluska B, Pashkow FJ, Stewart WJ. Influence of left ventricular hypertrophy on detection of coronary artery disease using exercise echocardiography. *J Am Coll Cardiol* 1995; **26:** 1180–1186.
7. Goldschlager N, Selzer A, Cohn K. Treadmill stress tests as indicators of presence and severity of coronary artery disease. *Ann Intern Med* 1976; **85:** 277–286.
8. Balow JB. The 'false positive' exercise electrocardiogram: Value of time course pattern in assessment of depressed ST segments and inverted T waves. *Am Heart J* 1985; **110:** 1328–1336.
9. Schartl M, Beckmann S, Bocksch W, Fateh-Mogham S, Fleck E. Stress echocardiography in special groups: In women, in left bundle branch block, in hypertension and after transplantation. *Eur Heart J* 1997; **18**(Suppl D): D63–D67.
10. Senior R, Basu S, Handler C, Raftery EB, Lahiri A. Diagnostic accuracy of dobutamine stress echocardiography for detection of coronary heart disease in hypertensive patients. *Eur Heart J* 1996; **17:** 289–295.
11. Bruce RA. Progress in exercise cardiology. *In*: Yu In, Goodwin F,

editors. Progress in cardiology, vol. 3. Philadelphia: Lea and Febiger; 1974; 113–172.
12. de Bruyne MC, Hoes AW, Kors JA, Hofman A, van Bemmel JH, Grobbee DE. QTc dispersion predicts cardiac mortality in the elderly: The Rotterdam Study. *Circulation* 1998; **97:** 467–472.
13. Sakuma T, Okada T, Hayashi Y, Otsuka M, Hirai Y. Optimal time for predicting left ventricular remodeling after successful primary coronary angioplasty in acute myocardial infarction using serial myocardial contrast echocardiography and magnetic resonance imaging. *Circ J* 2002; **66:** 685–690.
14. Yamada S, Mikami T, Komuro K, Onozuka H, Saito N, Nishihara K, et al. Sensitive method of detecting myocardial ischemia during dobutamine stress echocardiography. *Circ J* 2003; **67:** 317–322.
15. Hanley JA, McNeil BJ. A method of comparing the areas under receiver operating characteristic curves derived from the same cases. *Radiology* 1983; **148:** 839–843.
16. Rossi L, Carbonieri E, Castello C, Rossi R, Sciarretta G, Zardini P. Description and evaluation of the method for computer analysis of the exercise electrocardiogram. *J Electrocardiol* 1987; **20:** 77–85.
17. Robert AR, Melin JA, Dentry JMR. Logistic discrimination analysis improves diagnostic accuracy of exercise testing for coronary artery disease in women. *Circulation* 1991; **83:** 1202–1209.
18. Boronis PE, Greenberg PS, Castellanet MJ, Ellestad MH. Significance of changes in R wave amplitude during treadmill stress testing; angiographic correlation. *Am J Cardiol* 1978; **41:** 846–851.
19. Boronis PE, Greenberg PS, Christison GW, Castellanet MJ, Ellestad MH. Evaluation of R wave amplitude changes versus ST segment depression in stress testing. *Circulation* 1978; **57:** 904–910.
20. Detrtano R, Salcedo E, Passalacqua M, Friis R. Exercise electrocardiographic variables: A critical appraisal. *J Am Coll Cardiol* 1986; **8:** 836–847.
21. Kligfield P, Ameisen O, Okin PM. Heart rate adjustment of ST segment depression for improved detection of coronary artery disease. *Circulation* 1989; **79:** 245–255.
22. Okin PM, Kligfield P, Milner MR, Goldstein SA, Lindsay J. Heart rate adjustment of ST-segment depression for reduction of false positive electrocardiographic responses to exercise in asymptomatic men screened for coronary artery disease. *Am J Cardiol* 1988; **62:** 1043–1047.
23. Koide Y, Yotsukura M, Yoshino H, Ishikawa K. Value of QT dispersion in the interpretation of treadmill exercise electrocardiograms of patients without exercise-induced chest pain or ST-segment depression. *Am J Cardiol* 2000; **85:** 1094–1099.
24. Ascoop CA, Distelbrink CA, Delang PA. Clinical value of quantitive analysis of ST slope during exercise. *Br Heart J* 1977; **39:** 212–217.
25. Rodriguez M, Moussa I, Froning J, Kochumian M, Froelicher VF. Improved exercise test accuracy using discriminant function analysis and 'Recovery ST slope'. *J Electrocardiol* 1993; **26:** 207–218.
26. Ribisl PM, Morris CK, Kawaguchi T, Ueshima K, Froelicher VF. Angiographic patterns and severe coronary disease: Exercise test correlates. *Arch Intern Med* 1992; **152:** 1618–1624.
27. Ribisl PM, Liu J, Mousa I, Herbert WG, Miranda CP, Froning JN, et al. Comparison of computer ST criteria for diagnosis of severe coronary artery disease. *Am J Cardiol* 1993; **71:** 546–551.

Inhibition of Rho-Kinase in the Brainstem Augments Baroreflex Control of Heart Rate in Rats

Koji Ito, Yoshitaka Hirooka, Yoji Sagara, Yoshikuni Kimura, Kozo Kaibuchi, Hiroaki Shimokawa, Akira Takeshita, Kenji Sunagawa

Abstract—The Rho/Rho-kinase pathway in the nucleus tractus solitarii (NTS) of the brain stem contributes to blood pressure regulation. Activation of this pathway might be involved in the central nervous system mechanisms of hypertension. The aim of the present study was to determine whether baroreflex control of heart rate is altered by inhibition of Rho-kinase in the NTS. Adenovirus vectors encoding dominant-negative Rho-kinase or β-galactosidase were transfected into the nucleus tractus solitarii of Wistar Kyoto rats (WKY) and spontaneously hypertensive rats (SHR). Baroreflex control of heart rate was examined by changing arterial pressure with an intravenous infusion of phenylephrine or sodium nitroprusside. The maximum gain of baroreflex control of heart rate was attenuated in SHR compared with WKY before the gene transfer. Transfection of adenovirus vectors encoding dominant-negative Rho-kinase significantly augmented the maximum gain in both WKY and SHR. The extent of this augmentation, however, was greater in SHR than in WKY. After treatment with metoprolol, the maximum gain was significantly decreased in rats transfected with adenovirus vectors encoding dominant-negative Rho-kinase, but not in nontransfected rats. In contrast, after treatment with atropine, the maximum gain was greater in rats transfected with adenovirus vectors encoding dominant-negative Rho-kinase compared with nontransfected rats, although it was decreased in both groups. These results suggest that inhibition of Rho-kinase in the NTS augments baroreflex control of heart rate, in both WKY and SHR, probably because of a cardiac sympathoinhibitory effect. (***Hypertension.* 2004;44:478-483.)**

Key Words: blood pressure ■ heart rate ■ rho ■ hypertension ■ brain

It is well established that the arterial baroreceptor reflex is an important determinant of cardiovascular homeostasis.[1,2] The major baroreflex pathway is in the brain stem, and baroreceptor afferent inputs are initially integrated by neurons in the nucleus tractus solitarii (NTS).[3,4] Baroreflex control of heart rate (HR) is impaired in various animal models of hypertension as well as in hypertensive humans.[5-7] Furthermore, evidence suggests that many vasoactive substances, such as angiotensin II, affect sympathetic nerve activity and modulate the baroreflex control of HR and sympathetic nerve activity.[8,9]

The small GTPase, Rho, and its effector, Rho-kinase, are involved in various cellular functions, including myosin light chain phosphorylation and smooth muscle contraction.[10-12] Activation of this pathway contributes to the pathophysiology of hypertension.[13-15] We previously reported that Rho/Rho-kinase is present in the NTS and maintains arterial pressure via the sympathetic nervous system, and that activation of the Rho/Rho-kinase pathway in the NTS might contribute to the hypertensive mechanisms.[16,17] It is not known, however, whether Rho/Rho-kinase in the NTS is involved in baroreflex function. The Rho/Rho-kinase pathway in the central nervous system is involved in the maintenance of dendritic spines.[18] Dendritic spines form the postsynaptic contact sites of excitatory synapses in the central nervous system.[19,20] Therefore, the aim of the present study was to elucidate the role of the Rho/Rho-kinase pathway in the NTS in baroreflex control of HR in Wistar-Kyoto rats (WKY) and spontaneously hypertensive rats (SHR). For this purpose, adenovirus vectors encoding either dominant-negative Rho-kinase (AdDNRhoK) or β-galactosidase (Adβgal) were transfected into the NTS in vivo and mean arterial pressure (MAP)–HR curves were constructed using an intravenous infusion of phenylephrine or sodium nitroprusside to examine baroreflex function in WKY and SHR.

Methods

This study was approved by the Committee on Ethics of Animal Experiments, Kyushu University Graduate School of Medical Sciences, and conducted according to the Guidelines for Animal Experiments of Kyushu University. Male WKY or SHR (280 to 340 grams, 16 to 20 weeks old) were used in the present study. Rats were obtained from an established colony at the Animal Research Institute of Kyushu University Faculty of Medicine (Fukuoka, Japan).[13,17]

Received April 27, 2004; first decision May 14, 2004; revision accepted August 13, 2004.

From the Department of Cardiovascular Medicine (K.I., Y.H., Y.S., Y.K., H.S., A.T., K.S.), Kyushu University Graduate School of Medical Sciences, Fukuoka, Japan; Department of Cell Pharmacology (K.K.), Nagoya University Graduate School of Medicine, Nagoya, Japan.

Correspondence to Dr Yoshitaka Hirooka, Department of Cardiovascular Medicine, Kyushu University Graduate School of Medical Sciences, 3-1-1 Maidashi, Higashi-ku, Fukuoka 812-8582, Japan. E-mail hyoshi@cardiol.med.kyushu-u.ac.jp

Hypertension is available at http://www.hypertensionaha.org DOI: 10.1161/01.HYP.0000143120.24612.68

In Vivo Gene Transfer Experiments

Adenoviral vectors encoding either the β-galactosidase gene or the DNRhoK (Rho-binding domain of Rho-kinase) gene were used as described previously.[16] Systolic blood pressure (SBP) was measured before and at day 7 after gene transfer using the tail-cuff method. At day 7 after the gene transfer, we performed immunohistochemistry for c-myc, an AdDNRhoK tag protein, as described previously.[16]

Western Blot Analysis

We performed Western blot analysis for phosphorylated ERM (p-ERM) or total ERM family members (ezrin, radixin, moesin), which are target proteins of Rho-kinase[21] and membranous or total RhoA (1:1000; Santa Cruz Biotechnology) in the NTS of nontransfected rats as described previously.[16] Furthermore, we performed Western blot analysis for c-myc and p-ERM of brain tissue containing the injection sites in the NTS of AdDNRhoK-transfected rats before and at day 7 after gene transfer.[16]

Analysis of Baroreflex Control of HR

In AdDNRhoK-transfected rats or Adβgal-transfected rats, measurement of the sensitivity of baroreflex control of HR was performed on day 7 after the gene transfer.[16] Under pentobarbital anesthesia (40 mg/kg IP), catheters were inserted into the right femoral artery for measurement of blood pressure and HR, and into the femoral vein for infusion of phenylephrine or sodium nitroprusside. After animals awoke from the anesthesia, analysis of baroreflex control of HR was performed with animals in the conscious state. The femoral vein catheter was connected to an infusion pump and progressive infusion of phenylephrine (2 to 32 μg/kg per minute) at flow rates of 0.008 to 0.13 mL/min or sodium nitroprusside (5 to 10 μg/kg per minute) at flow rates of 0.007 to 0.013 mL/min for 1 minute was performed to induce changes in MAP between 40 and 50 mm Hg. The speed of the increase or decrease in MAP was ≈0.8 mm Hg per second.[7]

Some animals (hydralazine-treated WKY or SHR, n=5 for each) were treated with hydralazine hydrochloride in their drinking water (0.6 mg/mL) for 7 days. On day 7 after treatment with hydralazine, baroreflex control of HR was analyzed as described.

Effects of Autonomic Blockade

To examine the sympathetic and parasympathetic component of the interaction between Rho-kinase activity in the NTS and autonomic innervation of the sinoatrial node, metoprolol (a selective β_1-receptor blocker, 2 mg/kg IV, supplemented with 0.2 mg/kg IV every 30 minutes) or atropine methyl bromide[7,22] (0.2 mg/kg IV, supplemented with 0.02 mg/kg IV every 30 minutes) was injected in the nontransfected and AdDNRhoK-transfected rats. The measurement of the gain of baroreflex control of HR was performed as described previously.[7]

Data Analysis of Baroreflex Control of HR

To analyze the baroreflex control of HR, HR and MAP data were obtained every 2 seconds, and the relation between MAP and HR was determined by fitting pairs of data points to a logistic function using the computer program Igor Pro (Wave Metrics) as described previously.[7] The logistic function used for data analysis conformed to the mathematical expression $HR=P1/\{1+\exp[P2(MAP-P3)]\}+P4$, in which P1 is the range of responses of the HR, P2 is the slope coefficient, P3 is the MAP at the midpoint of the range for the HR, and P4 is the minimum HR. The maximum gain of baroreflex control of HR was expressed as $-P1\times P2/4$ of the logistic function curve.[7]

Statistical Analysis

All values are expressed as mean±SEM. Two-way ANOVA was used to compare the MAP and HR between the nontransfected and AdDNRhoK-transfected rats. Comparisons between any 2 mean values were performed using Bonferroni correction for multiple comparisons. An unpaired *t* test was used to compare the maximum gain of baroreflex control of HR between groups. Differences were considered statistically significant at $P<0.05$.

Results

Analysis of AdDNRhoK Expression in the NTS

Immunohistochemistry after AdDNRhoK transfection revealed c-myc expression locally in the NTS, where AdDNRhoK was microinjected (Figure 1A). In addition, Western blot analysis revealed that c-myc expression was significantly increased at day 7 after the transfection of AdDNRhoK in WKY and SHR (Figure 1B). The magnitude of the increase in c-myc expression did not differ between WKY and SHR (Figure 1B).

Effects of AdDNRhoK Transfection on Blood Pressure and HR

SBP and HR were significantly decreased on day 7 after the gene transfer of AdDNRhoK in SHR and WKY. The magnitude of the decrease in SBP and HR, however, was significantly greater in SHR than in WKY (ΔSBP: −39±4 versus −24±3 mm Hg; ΔHR: −98±8 versus −68±4 bpm; n=6 for each; $P<0.05$). In contrast, these variables did not change in either strain in nontransfected or Adβgal-transfected rats.[16] To confirm the specific inhibitory effects of AdDNRhoK transfection on Rho-kinase activity, we examined phosphorylation of the ERM family in rats transfected with AdDNRhoK into the NTS. Phosphorylation of the ERM family was significantly reduced in AdDNRhoK-transfected animals (Figure 1C).

Effects of Rho-Kinase Inhibition in the NTS on Baroreflex Control of HR

In the nontransfected group, the baroreflex curve shifted to the right and the maximum gain of baroreflex control of HR was significantly decreased in SHR compared with WKY(−0.8±0.1 versus −1.8±0.2; n=6 for each; $P<0.01$; Figure 2 A and 2B). In AdDNRhoK-transfected rats, the baroreflex curve shifted to the left and maximum gain of baroreflex control of HR was significantly increased compared with controls in both WKY (−2.7±0.3 versus −1.8±0.2; n=6 for each; $P<0.05$) and SHR (−2.0±0.2 versus −0.8±0.1; n=6 for each; $P<0.01$; Figure 2A and 2B). The magnitude of the augmentation of the maximum gain of baroreflex control of HR was significantly greater in SHR than in WKY (1.5±0.2 versus 2.5±0.1; data are expressed as relative ratio to the control group of each strain, which was assigned a value of 1). In Adβgal-transfected rats, none of the parameters was significantly different compared with those of nontransfected rats (data not shown).

Effects of Blood Pressure Reduction on Baroreflex Control of HR

In hydralazine-treated WKY (n=5), baseline MAP was significantly decreased compared with nontreated WKY (96±3 versus 116±3 mm Hg, $P<0.01$), and baseline HR was significantly increased (348±7 versus 323±7 bpm, $P<0.05$). There was no difference in the maximum gain of baroreflex control of HR between hydralazine-treated WKY and nontreated WKY (−1.7±0.2 versus −1.8±0.2; Figure 2C and 2D). In hydralazine-treated SHR (n=5), baseline MAP was significantly decreased compared with nontreated SHR (n=6) (123±5 versus 160±3 mm Hg; $P<0.01$), and baseline

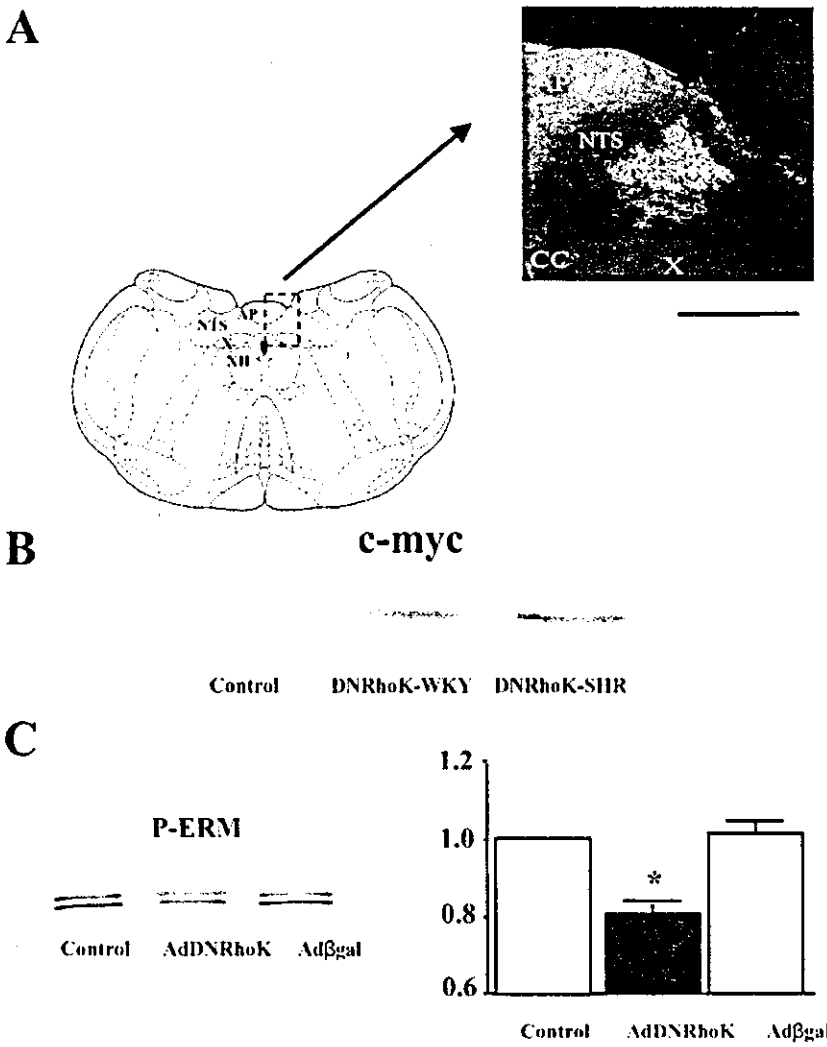

Figure 1. A, Histochemical analysis for site-specific c-myc expression within the NTS. Scale bar indicates 1 mm. B, Western blot analysis for c-myc in the medulla containing the NTS in WKY and SHR. The c-myc expression level in SHR was as same as in WKY. C, Western blot analysis for p-ERM, substrates of Rho-kinase before and after the gene transfer. The level of p-ERM was significantly reduced by the transfer of AdDNRhoK, but not by that of Adβgal.

HR was significantly increased (362±6 versus 339±4 bpm; $P<0.01$). The maximum gain of baroreflex control of HR was significantly increased in hydralazine-treated SHR compared with nontreated SHR (−1.1±0.1 versus −0.8±0.1; $P<0.05$), although the maximum gain of hydralazine-treated SHR was smaller than that in nontreated WKY (−1.8±0.2 versus −1.1±0.1; $P<0.01$; Figure 2C and 2D). Although hydralazine treatment produced a decrease in baseline blood pressure as did AdDNRhoK-transfection in SHR (baseline MAP 135±2 versus 123±5 mm Hg), the improvement in baroreflex control of HR was smaller in the hydralazine-treated SHR than in AdDNRhoK-transfected SHR.

Effects of Inhibition of Rho-Kinase in the NTS on Baroreflex Control of HR After Autonomic Blockade

In nontransfected WKY, atropine significantly increased the baseline HR (317±8 to 335±5 bpm; n=6 for each; $P<0.05$) and decreased the range of HR (113±13 to 53±8 bpm; $P<0.01$) and maximum gain of baroreflex control of HR (−1.8±0.2 to −0.9±0.1; $P<0.01$), but did not significantly change the baseline MAP (104±5 to 106±4 mm Hg; Figure 3A and 3B). Metoprolol significantly decreased the baseline HR (304±2 to 272±4 bpm; n=6 for each; $P<0.01$) and range of HR (113±13 to 32±4 bpm; $P<0.01$), and increased the slope coefficient (−0.07±0.02 to −0.23±0.03 bpm/mm Hg; $P<0.01$), but did not change the maximum gain of baroreflex control of HR (−1.8±0.2 to −1.7±0.2) and baseline MAP (107±6 to 107±6 mm Hg; Figure 3C and 3D). In AdDNRhoK-transfected WKY, atropine significantly decreased the range of HR (102±10 to 38±5 bpm; $P<0.01$) and maximum gain of baroreflex control of HR (−2.7±0.3 to −1.4±0.1; $P<0.01$), but did not alter the baseline MAP (89±4 to 89±4 mm Hg; n=6 for each). Baseline HR increased to 250±7 from 241±6 bpm, but this increase was not statistically significant (Figure 3A and 3B). Metoprolol significantly decreased baseline HR (243±2 to 220±4 bpm; $P<0.01$), the range of HR (102±10 to 60±10 bpm/min; $P<0.05$), and the maximum gain of baroreflex control of HR (−2.7±0.3 to −1.5±0.1; $P<0.01$), but did not alter the baseline MAP (90±2 to 86±2 mm Hg; Figure 3C and 3D). After treatment with atropine, the maximum gain of baroreflex control of HR was significantly greater in AdDNRhoK-transfected WKY than in nontransfected WKY (−1.4±0.3

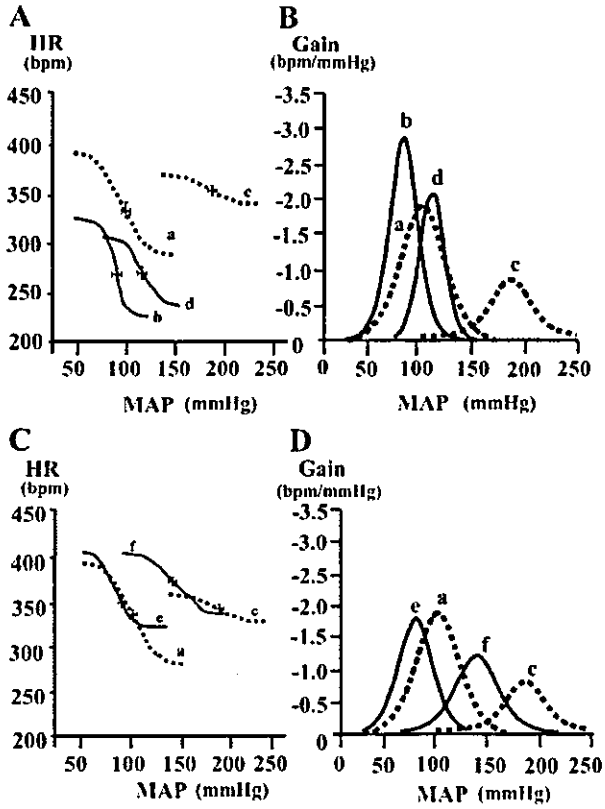

Figure 2. A, Average logistic function regression curves. B, Average gain curves; a indicates nontransfected WKY; b, AdDNRhoK-transfected WKY; c, nontransfected SHR; d, AdDNRhoK-transfected SHR; n=6 for each. C, Average logistic function regression curves. D, Average gain curves; e, nontransfected WKY treated with hydralazine; f, nontransfected SHR treated with hydralazine; n=6 for nontransfected animals and n=5 for hydralazine-treated animals.

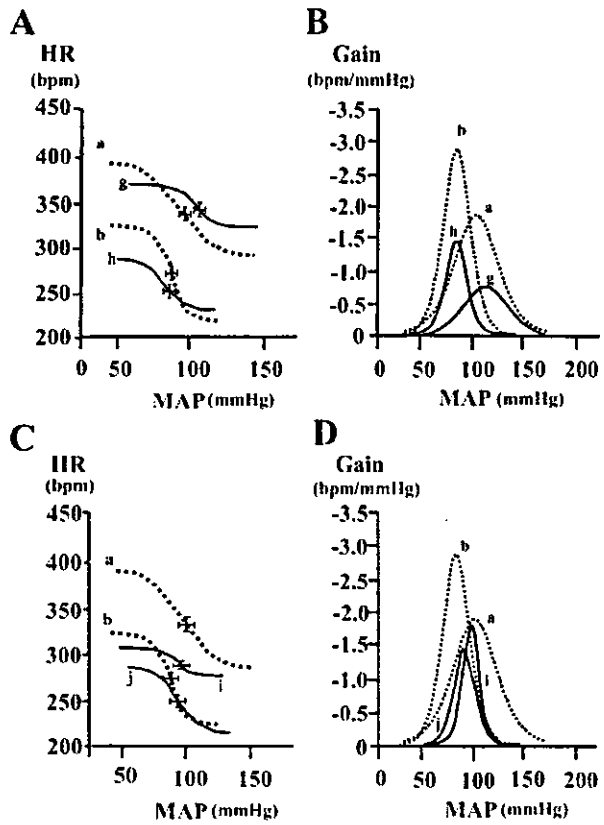

Figure 3. Average logistic function regression curves of the intravenous injection of atropine (A) or metoprolol (C). Average gain curves of the intravenous injection of atropine (B) or metoprolol (D); a indicates nontransfected WKY; b, AdDNRhoK-transfected WKY; g, nontransfected WKY injected with atropine intravenously; h, AdDNRhoK-transfected WKY injected with atropine intravenously; i, nontransfected WKY injected with metoprolol intravenously; j, AdDNRhoK-transfected WKY injected with metoprolol intravenously; n=6 for each.

versus -0.9 ± 0.1; $P<0.05$; Figure 3A and 3B). After treatment with metoprolol, however, the maximum gain of baroreflex control of HR was not different between AdDNRhoK-transfected and nontransfected WKY(-1.5 ± 0.1 versus -1.7 ± 0.2; Figure 3C and 3D).

Rho/Rho-Kinase Activity in the NTS

Expression of membranous RhoA, which represents RhoA activity,[23] was greater in SHR than in WKY (Figure 4 A). The expression level of membranous RhoA in hydralazine-treated SHR tended to decrease, but was not statistically different from that in nontreated SHR (Figure 4A). The level of p-ERM, which represents Rho-kinase activity,[21] was greater in SHR than in WKY (Figure 4 B). Furthermore, p-ERM family levels in hydralazine-treated SHR were significantly decreased compared with nontreated SHR, but significantly increased compared with nontreated WKY (Figure 4B).

Discussion

The present study demonstrated that inhibition of Rho-kinase in the NTS augments the baroreflex control of HR in WKY and SHR and improves the impaired baroreflex function in SHR. The major effect of Rho-kinase inhibition in the NTS on baroreflex control of HR appears to be caused by inhibition of the cardiac–sympathetic component.

In nontransfected SHR, the maximum gain of baroreflex control of HR was significantly decreased compared with nontransfected WKY, consistent with previous reports.[6,7] Inhibition of Rho-kinase activity in the NTS by AdDNRhoK increased the maximum gain in WKY and SHR; however, the magnitude of the augmentation of the maximum gain was significantly greater in SHR than in WKY. These results indicate that Rho-kinase in the NTS contributes to maintain baroreflex control of HR in both strains, and activation of this pathway contributes to impaired baroreflex control of HR in SHR. Consistent with this suggestion, RhoA and Rho-kinase activities were enhanced in the NTS of SHR compared with WKY, as shown in Figure 4. After treatment with atropine, the maximum gain was significantly decreased in both nontransfected WKY and AdDNRhoK-transfected WKY. Conversely, after treatment with metoprolol, the maximum gain was significantly decreased in only AdDNRhoK-transfected WKY. Furthermore, after treatment with atropine, the maximum gain was significantly greater in AdDNRhoK-transfected WKY than in nontransfected WKY, but after

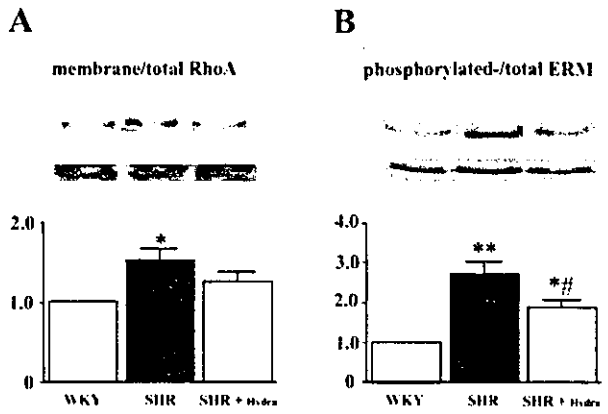

Figure 4. Protein expression of RhoA and p-ERM in the NTS. Data are expressed as relative ratio to WKY control, which was assigned a value of 1. A, The expression of RhoA in membrane and total RhoA. The graph shows the ratio of membranous RhoA to total RhoA. The RhoA protein level in the membrane fraction was significantly higher in SHR or hydralazine-treated SHR than in WKY (n=3). *$P<0.05$ versus WKY. B, The expression of p-ERM and total ERM. The graph shows the ratio of p-ERM to total ERM. The p-ERM expression level was significantly higher in SHR or hydralazine-treated SHR than in WKY (n=3). *$P<0.05$, **$P<0.01$ vs WKY, but the p-ERM expression level was significantly reduced in hydralazine-treated SHR compared with SHR (n=3). #$P<0.05$ vs SHR.

treatment with metoprolol, the maximum gain was not different between AdDNRhoK-transfected and nontransfected WKY. In the present study, we used adenovirus vectors, which might cause an inflammatory response. There is, however, no evidence that inflammation affects cardiovascular regulation.[16,24] These results suggest that gene transfer of AdDNRhoK into the NTS affects the cardiac sympathetic component of baroreflex function.[7]

There is a possibility that changes in arterial pressure by intravenous infusion of phenylephrine or sodium nitroprusside affect the cardiopulmonary receptors. The activity of the baroreceptors to pressure changes is decreased in animal models of hypertension.[25] Therefore, another experimental design, such as stimulation of the aortic depressor nerve, might be preferable. It is difficult to perform such an experiment in the awake rat, however, because the stimulating electrode must be implanted for a long period of time. However, the evaluation of the baroreflex function between normotensive and hypertensive models using phenylephrine or sodium nitroprusside has been widely used in previous studies.[26-28]

Rho-kinase inhibition in the NTS decreased arterial pressure, consistent with our previous report.[12] The decrease in blood pressure alone might affect baroreflex control of HR. Therefore, we examined the baroreflex control of HR in hydralazine-treated rats. In hydralazine-treated WKY, baseline MAP significantly decreased, but the maximum gain did not change compared with nontreated WKY, despite the fact that blood pressure decreased to a similar extent as in AdDNRhoK-transfected rats. In hydralazine-treated SHR, baseline MAP significantly decreased and the maximum gain was significantly increased compared with nontreated SHR, although the value of the maximum gain of hydralazine-treated SHR was smaller than in AdDNRhoK-transfected SHR, despite the fact that blood pressure decreased to a similar level as in AdDNRhoK-transfected SHR. These results indicate that the effects of Rho-kinase inhibition in the NTS on baroreflex function are not simply caused by the change in systemic blood pressure.

In conclusion, inhibition of endogenous Rho-kinase in the NTS augments the baroreflex control of HR in WKY and SHR and improves the impaired baroreflex function in SHR. The major effect of Rho-kinase inhibition in the NTS on baroreflex control of HR was probably caused by a cardiac sympatho-inhibitory effect.

Perspectives

The precise mechanisms by which Rho-kinase inhibition in the NTS augments the baroreflex control of HR cannot be determined from the results of our study. With regard to cardiovascular disease, the Rho/Rho-kinase pathway contributes to hypertension[13,15,29] and endothelial dysfunction.[30,31] The neuronal Rho/Rho-kinase pathway contributes to dendritic spine formation, which forms the postsynaptic contact site for the majority of excitatory synapses.[19,20,32] Recent studies demonstrate that morphological changes in dendritic spines occur rapidly[33] and are associated with glutamate sensitivity.[34] Furthermore, there are structural differences in dendritic spines in the NTS between WKY and SHR.[35] Therefore, the Rho/Rho-kinase pathway might affect synaptic transmission in the NTS. Further studies are needed to clarify the mechanisms underlying our observations.

Acknowledgments

This study was supported by grants-in-aid for Scientific Research (C13670721, C15590757) from the Ministry of Education, Culture, Sports, Science, and Technology of Japan, and by a grant for research on the autonomic nervous system and hypertension from Kimura Memorial Heart Foundation/Pfizer Pharmaceuticals, Inc.

References

1. Dampney RAL. Functional organization of central pathways regulating the cardiovascular system. *Physiol Rev.* 1994;74:323–364.
2. Pilowsky PM, Goodchild AK. Baroreceptor reflex pathways and neurotransmitters: 10 years on. *J Hypertens.* 2002;20:1675–1688.
3. Machado BH. Neurotransmission of the cardiovascular reflexes in the nucleus tractus solitarii of awake rats. *Ann N Y Acad Sci.* 2001;940:179–196.
4. Andresen MC. Nucleus tractus solitarius: gateway to neural circulatory control. *Annu Rev Physiol.* 1994;56:93–116.
5. Moreira ED, de Oliveria M, Krieger EM. Impaired baroreflex control of heart rate in high-renin renal hypertension. *J Hypertens.* 1988;6:619–625.
6. Gonzalez ER, Krieger AJ, Sapru HN. Central resetting of baroreflex in the spontaneously hypertensive rat. *Hypertension.* 1983;5:346–352.
7. Kishi T, Hirooka Y, Kimura Y, Sakai K, Ito K, Shimokawa H, Takeshita A. Overexpression of eNOS in RVLM improves impaired baroreflex control of heart rate in SHRSP. *Hypertension.* 2003;41:255–260.
8. Persson PB. Modulation of cardiovascular control mechanisms and their interaction. *Physiol Rev.* 1996;76:193–244.
9. Eshima K, Hirooka Y, Shigematsu H, Matsuo I, Koike G, Sakai K, Takeshita A. Angiotensin in the nucleus tractus solitarii contributes to neurogenic hypertension caused by chronic nitric oxide synthase inhibition. *Hypertension.* 2000;36:259–263.
10. Kimura K, Ito M, Amano M, Chihara K, Fukata Y, Nakafuku M, Yamamori B, Feng J, Nakano T, Okawa K, Iwamatsu A, Kaibuchi K. Regulation of myosin phosphatase by Rho and Rho-associate kinase (Rho-kinase). *Science.* 1996;273:245–248.

11. Kawano Y, Fukata Y, Oshiro N, Amano M, Nakamura T, Ito M, Matsumura F, Inagaki M, Kaibuchi K. Phosphorylation of myosin-binding subunit (MBS) of myosin phosphatase by Rho-kinase in vivo. *J Cell Biol.* 1999;147:1023–1037.
12. Kureishi Y, Kobayashi S, Amano M, Kimura K, Kanaide H, Nakano T, Kaibuchi K, Ito M. Rho-associated kinase directly induces smooth muscle contraction through myosin light chain phosphorylation. *J Biol Chem.* 1997;272:12257–12260.
13. Mukai Y, Shimokawa H, Matoba T, Kandabashi T, Satoh S, Hiroki J, Kaibuchi K, Takeshita A. Involvement of Rho-kinase in hypertensive vascular disease: a novel therapeutic target in hypertension. *FASEB J.* 2001;15:1062–1064.
14. Seko T, Ito M, Kureishi Y, Okamoto R, Moriki N, Onishi K, Isaka N, Hartshorne DJ, Nakano T. Activation of RhoA and inhibition of myosin phosphatase as important components in hypertension in vascular smooth muscle. *Circ Res.* 2003;92:411–418.
15. Masumoto A, Hirooka Y, Shimokawa H, Hironaga K, Setoguchi S, Takeshita A. Possible involvement of Rho-kinase in the pathogenesis of hypertension in humans. *Hypertension.* 2001;38:1307–1310.
16. Ito K, Hirooka Y, Sakai K, Kishi T, Kaibuchi K, Shimokawa H, Takeshita A. Rho/Rho-kinase pathway in brain stem contributes to blood pressure regulation via sympathetic nervous system: possible involvement in neural mechanisms of hypertension. *Circ Res.* 2003;92:1337–1343.
17. Ito K, Hirooka Y, Kishi T, Kimura Y, Kaibuchi K, Shimokawa H, Takeshita A. Rho/Rho-kinase pathway in the brainstem contributes to hypertension caused by chronic nitric oxide synthase inhibition. *Hypertension.* 2004;43:156–162.
18. Nakayama AY, Harms MB, Luo L. Small GTPases Rac and Rho in the maintenance of dendritic spines and branches in hippocampal pyramidal neurons. *J Neurosci.* 2000;20:5329–5338.
19. Koch C, Zador A. The function of dendritic spines: devices subserving biochemical rather than electrical compartmentalization. *J Neurosci.* 1993;13:413–422.
20. Nakazawa T, Watabe AM, Tezuka T, Yoshida Y, Yokoyama K, Umemori H, Inoue A, Okabe S, Manabe T, Yamamoto T. p250GAP, a novel brain-enriched GTPase-activating protein for Rho family GTPases, is involved in the N-methyl-D-aspartate receptor signaling. *Mol Biol Cell.* 2003;14:2921–2934.
21. Matsui T, Maeda M, Doi Y, Yonemura S, Amano M, Kaibuchi K, Tsukita S. Rho-kinase phosphorylate COOH-terminal threonines of Ezrin/Radixin/Moesin (ERM) proteins and regulates their head-to-tail association. *J Cell Biol.* 1998;140:647–657.
22. Liu JL, Murakami H, Zucker IH. Angiotensin II-Nitric oxide interaction on sympathetic outflow in conscious rabbits. *Circ Res.* 1998;82:496–502.
23. Liao JK, Homey CJ. Specific receptor-guanine nucleotide binding protein interaction mediates the release of endothelium-derived relaxing factor. *Circ Res.* 1992;70:1018–1026.
24. Sakai K, Hirooka Y, Matsuo I, Eshima K, Shigematsu H, Shimokawa H, Takeshita A. Overexpression of eNOS in NTS causes hypotension and bradycardia in vivo. *Hypertension.* 2000;36:1023–1028.
25. Chapleau MW, Li Z, Meyrelles SS, Ma X, Abboud FM. Mechanisms determining sensitivity of baroreceptor afferents in health and disease. *Ann N Y Acad Sci.* 2001;940:1–19.
26. Matsumura K, Averill DB, Ferrario CM. Angiotensin II acts at AT1 receptors in the nucleus of the solitary tract to attenuate the baroreceptor reflex. *Am J Physiol.* 1998;275:R1611–R1619.
27. Talman WT, Dragon DN. Transmission of arterial baroreflex signals depends on neural nitric oxide synthase. *Hypertension.* 2004;43:820–824.
28. Nishizawa M, Kumagai H, Ichikawa M, Oshima N, Suzuki H, Saruta T. Improvement in baroreflex function by an oral angiotensin receptor antagonist in rats with myocardial infarction. *Hypertension.* 1997;29:458–463.
29. Wettschureck N, Offermenns S. Rho/Rho-kinase mediated signaling in physiology and pathophysiology. *J Mol Med.* 2002;80:629–638.
30. Hernandez-Perera O, Perez-Sala D, Soria E, Lamas S. Involvement of Rho GTPases in the transcriptional inhibition of preproendothelin-1 gene expression by simvastatin in vascular endothelial cells. *Circ Res.* 2000;87:616–622.
31. Eto M, Barandier C, Rathgeb L, Kozai T, Joch H, Yang Z, Luscher TF. Thrombin suppresses endothelial nitric oxide synthase and upregulates endothelin-converting enzyme-1 expression by distinct pathways: role of Rho/ROCK and mitogen-activated protein kinase. *Circ Res.* 2001;89:583–590.
32. Van Aelst L, Cline HT. Rho GTPases and activity-dependent dendrite development. *Curr Opin Neurobiol.* 2004;14:297–304.
33. Fischer M, Kaech S, Knutti D, Matus A. Rapid actin-based plasticity in dendritic spines. *Neuron.* 1998;20:847–854.
34. Matsuzaki M, Ellis-Davies GC, Nemoto T, Miyashita Y, Iino M, Kasai H. Dendritic spine geometry is critical for AMPA receptor expression in hippocampal CA1 pyramidal neurons. *Nat Neurosci.* 2001;4:1086–1092.
35. Aicher SA, Sharma S, Mitchell JL. Structural changes in AMPA-receptive neurons in the nucleus of the solitary tract of spontaneously hypertensive rats. *Hypertension.* 2003;41:1246–1252.

Rapid Communication

Bone Marrow–Derived Monocyte Chemoattractant Protein-1 Receptor CCR2 Is Critical in Angiotensin II–Induced Acceleration of Atherosclerosis and Aneurysm Formation in Hypercholesterolemic Mice

Minako Ishibashi, Kensuke Egashira, Qingwei Zhao, Ken-ichi Hiasa, Kisho Ohtani, Yoshiko Ihara, Israel F. Charo, Shinobu Kura, Teruhisa Tsuzuki, Akira Takeshita, Kenji Sunagawa

Abstract—Angiotensin II (Ang II) is implicated in atherogenesis by activating inflammatory responses in arterial wall cells. Ang II accelerates the atherosclerotic process in hyperlipidemic apoE−/− mice by recruiting and activating monocytes. Monocyte chemoattractant protein-1 (MCP-1) controls monocyte-mediated inflammation through its receptor, CCR2. The roles of leukocyte-derived CCR2 in the Ang II-induced acceleration of the atherosclerotic process, however, are not known. We hypothesized that deficiency of leukocyte-derived CCR2 suppresses Ang II-induced atherosclerosis.

Methods and Results—A bone marrow transplantation technique (BMT) was used to develop apoE−/− mice with and without deficiency of CCR2 in leukocytes (BMT-apoE−/−CCR2+/+ and BMT-apoE−/−CCR2−/− mice). Compared with BMT-apoE−/−CCR2+/+ mice, Ang II-induced increases in atherosclerosis plaque size and abdominal aortic aneurysm formation were suppressed in BMT-apoE−/−CCR2−/− mice. This suppression was associated with a marked decrease in monocyte-mediated inflammation and inflammatory cytokine expression.

Conclusion—Leukocyte-derived CCR2 is critical in Ang II-induced atherosclerosis and abdominal aneurysm formation. The present data suggest that vascular inflammation mediated by CCR2 in leukocytes is a reasonable target of therapy for treatment of atherosclerosis. (*Arterioscler Thromb Vasc Biol.* 2003;24:e174–e178.)

Key Words: atherosclerosis ■ angiotensin II ■ inflammation ■ leukocytes

Web Site Feature

The full-length article can be found on the World Wide Web at http://www.atvbaha.org.

Excessive Increase in QT Interval and Dispersion of Repolarization Predict Recurrent Ventricular Tachyarrhythmia after Amiodarone

TAKESHI AIBA,*† WATARU SHIMIZU,* MASASHI INAGAKI,† KAZUHIRO SATOMI,* ATSUSHI TAGUCHI,* TAKASHI KURITA,* KAZUHIRO SUYAMA,* NAOHIKO AIHARA,* KENJI SUNAGAWA,† and SHIRO KAMAKURA*

From the *Division of Cardiology, Department of Internal Medicine, and the †Department of Cardiovascular Dynamics, Research Institute, National Cardiovascular Center, Suita, Japan

AIBA, T., ET AL.: Excessive Increase in QT Interval and Dispersion of Repolarization Predict Recurrent Ventricular Tachyarrhythmia after Amiodarone. *Although chronic amiodarone has been proven to be effective to suppress ventricular tachycardia (VT) and ventricular fibrillation (VF), how we predict the recurrence of VT/VF after chronic amiodarone remains unknown. This study evaluated the predictive value of the QT interval, spatial, and transmural dispersions of repolarization (SDR and TDR) for further arrhythmic events after chronic amiodarone. Eighty-seven leads body surface ECGs were recorded before (pre) and one month after (post) chronic oral amiodarone in 50 patients with sustained monomorphic VT associated with organic heart disease. The Q-Tend (QTe), the Q-Tpeak (QTp), and the interval between Tpeak and Tend (Tp-e) as an index of TDR were measured automatically from 87-lead ECG, corrected Bazett's method (QTce, QTcp, Tcp-e), and averaged among all 87 leads. As an index of SDR, the maximum (max) minus minimum (min) QTce (max-min QTce) and standard deviation of QTce (SD-QTce) was obtained among 87 leads. All patients were prospectively followed (15 ± 10 months) after starting amiodarone, and 20 patients had arrhythmic events. The univariate analysis revealed that post max QTce, post SD-QTce, post max-min QTce, and post mean Tcp-e from 87-lead but not from 12-lead ECG were the significant predictors for further arrhythmic events. ROC analysis indicated the post max-min QTce ≥106 ms as the best predictor of events (hazard ratio = 10.4, 95%, CI 2.7 to 40.5, P = 0.0008). Excessive QT prolongation associated with increased spatial and transmural dispersions of repolarization predict the recurrence of VT/VF after amiodarone treatment. (PACE 2004; 27:901–909)*

amiodarone, QT interval, dispersion, ventricular tachycardia, prognosis

Introduction

Spatial heterogeneity of ventricular repolarization has been important as the genesis of ventricular tachyarrhythmias.[1] The QT dispersion and recovery time dispersion, which are assumed to reflect the spatial heterogeneity,[2,3] have been proposed as a marker of electrical instability under several conditions, such as congenital long QT syndrome (LQTS).[4–9] On the other hand, recent experimental studies have suggested that transmural dispersion of repolarization (TDR) across the ventricular wall (epicardial, midmyocardial (M), and endocardial cells) was linked to ventricular arrhythmias such as torsades de pointes (TdP) under LQTS conditions.[10–12] The peak and the end of the T wave in the ECG are reported to coincide with repolarization of the epicardial and the longest M cell action potentials, respectively,[13] so that the interval between the Tpeak and Tend (Tp-e) is expected to reflect TDR.[14,15]

Chronic amiodarone therapy reduced slowly activating delayed rectifier K^+ currents (I_{Ks}) in the ventricular myocardium,[16] resulting in prolongation of action potential duration and suppression of life-threatening tachyarrhythmia in patients with structural heart disease.[17] Although amiodarone is classified into Class III antiarrhythmic agents, TdP is rare due to homogeneous prolongation of regional ventricular repolarization (QT interval).[18,19] Previous studies have attempted to show the effect of amiodarone on the QT interval and QT dispersion in the standard 12-lead electrocardiogram (ECG).[20–22] However, the change of QT dispersion after amiodarone therapy was

Dr. Shimizu was supported in part by the Japanese Cardiovascular Research Foundation, Vehicle Racing Commemorative Foundation, and Health Sciences Research Grants from the Ministry of Health, Labor and Welfare, and Research Grant for Cardiovascular Diseases (15C-6) from the Ministry of Health, Labor and Welfare, Japan.

Presented in part at the 24th North American Society of Pacing and Electrophysiology (NASPE) meeting, Washington DC, May 14, 2003, and published as an abstract (PACE 2003; 26:998).

Wataru Shimizu, M.D., Division of Cardiology, Department of Internal Medicine, National Cardiovascular Center, 5-7-1 Fujishiro-dai, Suita, Osaka, 565-8565 Japan. Fax: 81-6-6872-7486; e-mail: wshimizu@hsp.ncvc.go.jp

Received August 12, 2003; revised February 19, 2004; accepted March 2, 2004.

controversial. Moreover, the effect of amiodarone therapy on TDR was reported only in some experimental studies,[23–25] but not in a clinical study. In the present study, we measured the spatial and transmural dispersions of repolarization obtained from the 87-lead body surface mapping ECG before and 1 month after starting oral amiodarone, and investigated the predictive value of these repolarization parameters for recurrence of ventricular tachyarrhythmias. Our results suggested that excessive prolongation of the maximum QTc interval associated with increased spatial and transmural dispersions of repolarization predicted the risk of further arrhythmic events after amiodarone.

Methods

Patient Population

We prospectively investigated 50 patients (39 men, 11 women) with a mean age of 57 ± 10 years (Table I), who had been referred to the National Cardiovascular Center between 1993 and 2001. All patients had a history of symptomatic sustained monomorphic ventricular tachycardia (VT) associated with prior myocardial infarction (22 patients), dilated cardiomyopathy (21 patients), and arrhythmogenic right ventricular cardiomyopathy (7 patients). Mean left ventricular ejection fraction (LVEF) was 31% ± 12%, and 47 (94%) patients were in New York Heart Association functional class (NYHA) I or II. All patients were in sinus rhythm, and had no complete right or left bundle branch block. They received oral amiodarone with loading dose of 300 or 400 mg/day for two weeks followed by maintenance dose of 150 or 200 mg/day. Dose or type of β-blockers, angiotensin converting enzyme inhibitor, and other cardiac active drugs were not changed in all patients during the follow-up periods. The other antiarrhythmic medications were discontinued for at least five drug half-lives before administration of oral amiodarone. The median follow-up periods before amiodarone treatment were 5 months (1-156 months) and the incidence of pretreatment VT was 0.50 times (0.06-2.0)/month. The protocol of this study was explained to all patients, and informed consent was obtained from all patients.

Table I.
Patients Characteristics

Patients (n)	50
Age (yrs)	57 (10)
Gender (Men)	39
Basal disease (n)	
prior MI	22
DCM	21
ARVC	7
NYHA (I/II/III)	19/28/3
LVEF (%)	31 (12)
VT rate (/min)	188 (29)
Medication [n (%)]	
ACE-I	23 (46%)
β-blocker	17 (34%)
digitalis	14 (28%)
ICD (%)	15 (30%)

The data of Age, LVEF, and VT rate are presented as the mean value (SD).
ACE-I = angiotensin converting enzyme inhibitor; ARVC = arrhythmogenic right ventricular cardiomyopathy; DCM = dilated cardiomyopathy; LVEF = left ventricular ejection fraction; MI = myocardial infarction; NYHA = New York Heart Association functional class; VT = ventricular tachycardia.

Measurements of the 87-Lead Body Surface ECG

Eighty-seven-lead body surface ECG and standard 12-lead ECG were simultaneously recorded with a VCM-3000 (Fukuda Denshi Co., Tokyo, Japan) before (pre) and 1 month after (post) starting oral amiodarone in all patients. The method for recording have been detailed in previous studies.[8,14,15] These ECG data were simultaneously digitized at 1.0 kHz in each channel, stored on a floppy disk, and transferred to a personal computer with the analysis program developed by our institution. The 87-lead and 12-lead ECGs were analyzed using an automatic digitized program. The Q-Tend interval (QTe) was defined as the time interval between the QRS onset and the point at which the isoelectric line intersected a tangential line drawn at the minimum first derivative (dV/dt) point of the positive T wave or at the maximum dV/dt point of the negative T wave. When a bifurcated or secondary T wave (pathological U wave) appeared, it was included as part of the measurement of the QT interval, but a normal U wave, which was apparently separated from T wave, was not included. The Q-Tpeak interval (QTp) was defined as the time interval between the QRS onset and the point at the peak of positive T wave or the nadir of the negative T wave. When a T wave had a biphasic or a notched configuration, peak of the T wave was defined as that of the dominant T wave deflection. If the end and peak of the T wave was unidentifiable because of the flat or low amplitude T wave (amplitude < 0.05 mV), the lead was excluded. The QTe, the QTp, as well as the Tp-e (QTe minus QTp) as an index of TDR were measured automatically from all 87-lead ECGs, corrected to heart rate by Bazett's method (QTce, QTcp, Tcp-e: QTe/$\sqrt{RR}$, QTp/$\sqrt{RR}$, Tp-e/$\sqrt{RR}$), and averaged among 87 leads. Each point determined by the computer was checked visually for each lead. As an index of spatial dispersion of repolarization (SDR), the maximum

minus minimum of the QTce (max-min QTce) and standard deviation of the QTce (SD-QTce) among all 87 leads was also measured.

Follow-Up

Patients were prospectively followed for a maximum of 24 months after the second ECG recording during oral amiodarone. The endpoint was recurrence of sustained VT, ventricular fibrillation (VF), or sudden cardiac death. Sustained VT was defined as a tachycardia of ventricular origin at a rate of >100 beats/min and lasting for >30 seconds or resulting in hemodynamic collapse. No patients received any antiarrhythmic drugs other than oral amiodarone during the follow-up periods. The relationship between the repolarization parameters obtained from 12- and 87-lead and subsequent arrhythmic events was investigated.

Statistical Analysis

Data are expressed as mean ± SD for continuous variables and percentage for categorical variables, and compared by the paired *t* test. Univariate predictors of arrhythmic events were evaluated using the Cox proportional hazard model. Multivariate Cox models were used to test the independence of significant factors by univariate Cox regression analysis, including clinical variables. The receiver operating characteristics (ROC) curves, which analyze the sensitivity as the function of the complement of specificity, were used to evaluate the accuracy of the repolarization parameters. Event-free curves were generated using the Kaplan-Meier method, and compared by the log-rank test. A value of $P < 0.05$ was considered statistically significant.

Results

Change of Repolarization Parameters with Chronic Amiodarone

Figure 1 illustrates superimposed 87-lead ECGs before and after amiodarone in two cases. In the first case (panel A), the max and min QTce interval after amiodarone were similar to those before amiodarone, thus the max-min QTce, SD-QTce, and mean Tcp-e were not increased after amiodarone. On the other hand, in another case (panel B), the max QTce was remarkably prolonged after amiodarone compared to the min QTce, resulting in increasing the max-min QTce, SD-QTce, and mean Tcp-e.

Table 2 summarized the change of repolarization parameters with amiodarone in all patients. The RR interval was significantly prolonged after amiodarone, whereas QRS duration was not changed. Among 12-lead ECG, although both the

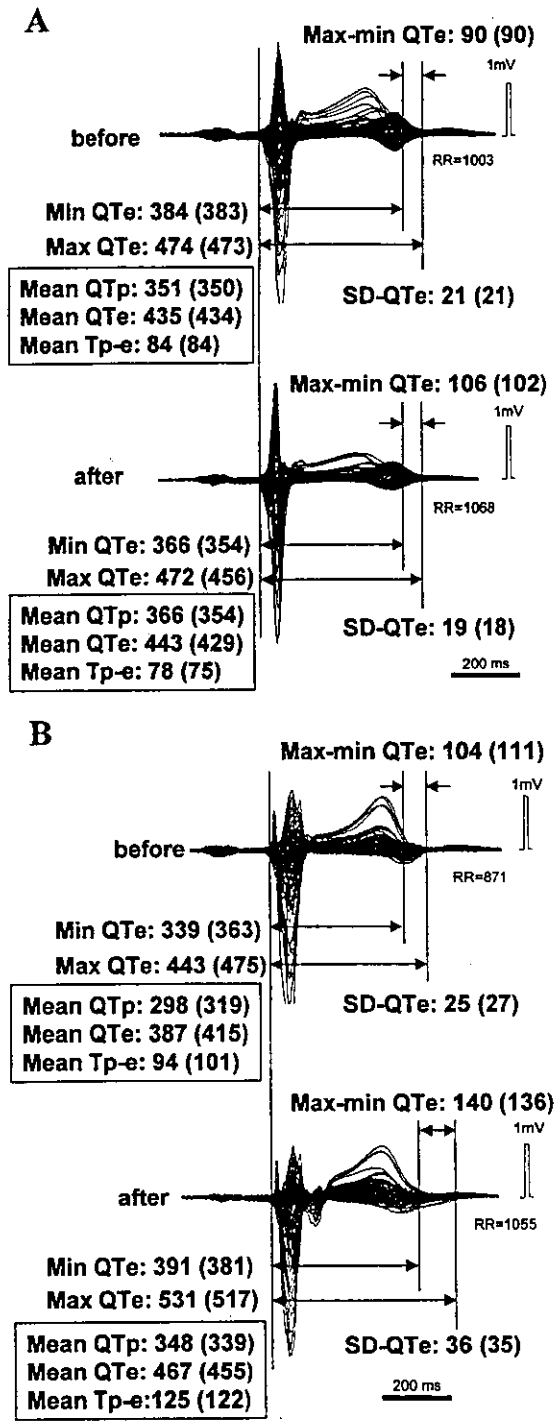

Figure 1. *The superimposed 87-lead ECGs before and after amiodarone in two cases (A and B). All data are presented in ms. Max = maximum value among 87 leads; Min = minimum value among 87 leads; QTe = Q-Tend interval; QTp = Q-Tpeak interval; Tp-e = Tpeak-Tend interval; Max-min QTe = difference between max QTe and min QTe; SD-QTe = standard deviation of QTe among 87 leads; Mean = average value among 87 leads. ( ) = corrected to heart rate by Bazett's method.*

Table II.

Change of Parameters with Chronic Amiodarone

		Before	After	P
	RR	936 ± 137	1017 ± 130	<0.01
	QRS	111 ± 27	120 ± 31	0.14
12-lead	Max QTce	457 ± 41	511 ± 68	<0.01
	Min QTce	394 ± 45	431 ± 49	<0.01
	Max-Min QTce	64 ± 37	80 ± 43	0.053
	SD-QTce	20 ± 13	24 ± 13	0.11
	V5 Tcp-e	90 ± 27	108 ± 45	<0.01
87-lead	Max QTce	470 ± 40	522 ± 60	<0.01
	Min QTce	374 ± 30	400 ± 39	<0.01
	Max-Min QTce	96 ± 30	122 ± 43	<0.01
	SD-QTce	19 ± 7	26 ± 12	<0.01
	Mean QTce	425 ± 37	463 ± 46	<0.01
	Mean QTcp	341 ± 31	363 ± 35	<0.01
	Mean Tcp-e	85 ± 13	101 ± 26	<0.01

All data are presented as the mean ± SD in ms. Max = maximum value among 12 or 87 lead; Min = minimum value among 12 or 87 leads; QTce = corrected Q-Tend interval; Max-Min QTce = maximum minus minimum QTce; SD-QTce = standard deviation of QTce among 12 or 87 leads; QTcp = corrected Q-Tpeak interval; Tcp-e = corrected Tpeak-Tend interval.

max and min QTce were significantly prolonged after amiodarone, the max-min QTce and SD-QTce were not significantly changed (P = 0.053 and P = 0.11, respectively). Among 87-lead ECG, both the max and min QTce were also significantly prolonged after amiodarone; the max QTce was more prolonged compared to the min QTce, thus significantly increasing the max-min QTce and SD-QTce. Moreover, both the mean QTce and mean QTcp were significantly prolonged after amiodarone; the mean QTce was more prolonged compared to the mean QTcp, thus significantly increasing the mean Tcp-e.

Clinical Outcome

Mean follow-up period was 15 ± 10 months after the second recording of body surface ECG during oral amiodarone. The arrhythmic events occurred in 20 of 50 (40%) patients, however no patients had proarrhythmia. Three patients suddenly died, probably due to VT, and the other 17 patients developed recurrence of sustained monomorphic VT. The recurrent VT had the same QRS morphology as those documented before administrating amiodarone in 15 of the 17 patients. We discontinued treating with amiodarone in 11 of the 17 patients as a result of recurrent VT. There was no difference in the amiodarone loading and maintenance doses between patients with (353 ± 78 mg/day and 197 ± 32 mg/day, respectively) and without (374 ± 81 mg/day and 194 ± 34 mg/day, respectively) recurrence of VT/VF. We implanted an implantable cardioverter defibrillator (ICD) in 15 (30%) of the 50 patients, and VT was detected by ICD in 6 (40%) of the 15 patients. In the remaining 35 patients without ICD, 14 (40%) patients had recurrence of VT or died suddenly. Thus, there is no detection bias for the arrhythmic events between patients with and without ICD. Moreover, there was no significant difference in the clinical outcome between patients with prior myocardial infarction, dilated cardiomyopathy, and arrhythmogenic right ventricular cardiomyopathy.

Predictors of Arrhythmic Events

Univariate predictors of arrhythmic events are shown in Table III. Age, gender, basal heart disease, LVEF, NYHA functional class, previous VT rate, and medical treatments were not related to further arrhythmic events. No parameters from the 12-lead ECGs were significantly correlated to further arrhythmic events. However, repolarization parameters from the 87-lead ECG, such as post max QTce, post max-min QTce, post SD-QTce, and post mean Tcp-e, were significantly correlated to further arrhythmic events. The ROC analysis showed that these repolarization parameters from the 87-lead ECG were superior to those from the 12-lead ECG, and the post max-min QTce from 87-lead was the strongest parameter to predict further arrhythmic events (Fig. 2). Moreover, the ROC curves indicated the post max QTce of 510 ms, post max-min QTce of 106 ms, post SD-QTce of 22.4 ms, and post mean Tcp-e of 100 ms as the best cutoff point of each parameters.

For the multivariate Cox analysis, clinical variables (age, gender, basal heart disease, LVEF) and the post max-min QTce from the 87-lead ECG, which was the strongest predictor for arrhythmic events, were entered as independent categorical variables. As a result, post max-min QTce ≥106 ms was a significant predictor of further arrhythmic events after amiodarone treatment (hazard ratio = 10.4, 95%CI: 2.7 to 40.5, P = 0.0008). Kaplan-Meier event-free probability curves showed that patients with post max QTce ≥510 ms had higher arrhythmic events after amiodarone than those < 510 ms (P = 0.0003, Fig. 3A). Similarly, patients with post max-min QTce ≥106 ms, post SD-QTce ≥22.4 ms or post mean Tcp-e ≥100 ms had highly arrhythmic events than those <106 ms, <22.4 ms, or <100 ms (P < 0.0001, P = 0.0007, and P = 0.002, respectively. Fig. 3B, 3C, 3D). The sensitivity, specificity, positive and negative predictive values, and accuracy in these

Table III.

Univariate Analysis of Arrhythmic Events after Chronic Amiodarone

Variables	Parameter Estimate	Hazard Ratio	95% CI	P value
Age	0.015	1.02	0.97–1.06	0.50
Gender (M)	0.010	1.01	0.34–3.02	0.98
Prior MI	0.085	1.09	0.45–2.63	0.85
LVEF < 30%	0.175	1.19	0.49–2.92	0.70
NHYA ≥ 2	0.356	1.43	0.55–3.73	0.47
VT rate	−0.011	0.99	0.97–1.01	0.20
ACE-I	−0.454	0.64	0.25–1.61	0.34
β-blocker	−0.459	0.63	0.23–1.78	0.38
digitalis	0.396	1.49	0.58–3.84	0.41
pre-Max QTce (/ms)	0.005	1.005	0.99–1.02	0.39
post-Max QTce (/ms)	0.007	1.007	1.00–1.01	0.008
pre-Min QTce (/ms)	0.005	1.005	0.99–1.02	0.49
post-Min QTce (/ms)	0.002	1.002	0.99–1.01	0.72
pre-Max-Min QTce (/ms)	0.003	1.003	0.99–1.02	0.63
post-Max-Min QTce (/ms)	0.015	1.015	1.01–1.02	0.0005
pre-SD-QTce (/ms)	0.008	1.008	0.95–1.07	0.79
post-SD-QTce (/ms)	0.04	1.04	1.01–1.07	0.007
pre-Mean QTce (/ms)	0.004	1.004	0.99–1.02	0.52
post-Mean QTce (/ms)	0.007	1.007	0.99–1.02	0.07
pre-Mean QTcp (/ms)	0.003	1.00	0.99–1.02	0.68
post-Mean QTcp (/ms)	0.004	1.00	0.99–1.02	0.56
pre-Mean Tcp-e (/ms)	0.016	1.02	0.98–1.05	0.37
post-Mean Tcp-e (/ms)	0.018	1.018	1.01–1.03	0.004

pre = before amiodarone; post = after amiodarone. Abbreviations as in Table I and Table II.

parameters for further arrhythmic events were shown in Table IV.

Change of Dispersions and VT/VF Recurrence

Figure 4 illustrates a scatter plot of the data about changes of max-min QTce (ΔSDR) and mean Tcp-e (ΔTDR) with amiodarone in patients with and without recurrence of VT/VF. The ΔSDR and ΔTDR were significantly larger in patients with VT/VF recurrence after amiodarone than those with no recurrence of VT/VF (49 ± 34 ms vs 8 ± 33 ms; $P < 0.001$, and 27 ± 34 ms vs 8 ± 15 ms; $P < 0.05$, respectively).

Discussion

Effect of Amiodarone on Spatial and Transmural Dispersion of Repolarization

Amiodarone is one of the most potent antiarrhythmic drugs in preventing life-threatening arrhythmias.[17] Several clinical studies demonstrated that amiodarone prolonged the QT (QTc) interval but did not increase QT (QTc) dispersion,[20–22] contributing to a very low incidence of TdP arrhythmias.[18,19] Experimental studies in dog model by van Opstal et al.[19] and in isolated rabbit heart by Zabel et al.[26] suggested that the low incidence of TdP with amiodarone was due to the homogenous local ventricular repolarization. However, the standard 12-lead ECG had too small number of leads to cover the whole area of body surface, therefore QT (QTc) dispersion from the 12-lead ECG could not always reflect spatial dispersion of local ventricular repolarization from the whole heart. Our results showed that the baseline max-min QTce obtained from the 87-lead ECG was larger than that from the 12-lead ECG. Therefore, the 87-lead body surface ECGs might reflect in more detail the spatial heterogeneity of ventricular repolarization. Moreover, our results showed that the max-min QTce and SD-QTce was increased after amiodarone in patients with VT/VF recurrence but not in patients without VT/VF recurrence, which may represent the arrhythmogeneity of the increase in SDR.

Recent experimental studies under long QT conditions suggested that increasing TDR across the ventricular wall was linked to ventricular

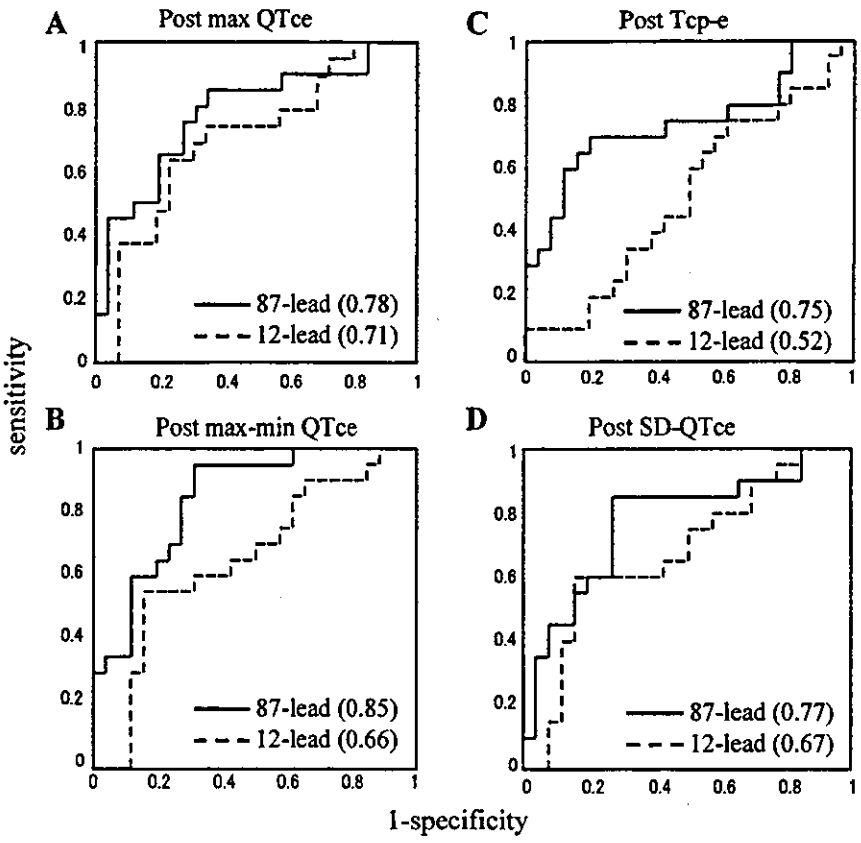

Figure 2. *Receiver operating characteristics curves for the post max QTce, post max-min QTce, post Tcp-e, and post SD-QTce from 87-lead ECG (solid line) and the 12-lead ECG (dotted line) in predicting arrhythmic events after amiodarone. ( ) = area of under curve.*

arrhythmias,[10–12] and that the Tp-e interval in the transmural ECG reflected TDR.[13] Previous experimental studies reported that chronic amiodarone reduced TDR in canine and human hearts.[23,24] These findings suggested that the decrease in TDR with chronic amiodarone, may in part contribute to its antiarrhythmic effect as well as low incidence of proarrhythmias. This study is the first one to demonstrate the change of Tcp-e interval with chronic oral amiodarone, showing that chronic amiodarone slightly but significantly increased the mean Tcp-e, which may relate to the arrhythmogenesis. However, our data also suggested that the mean Tcp-e was not so much increased in patients without VT/VF recurrence after amiodarone compared to those with VT/VF recurrence (Fig. 4). These results are consistent with the report by Merot et al.[25] that chronic amiodarone induced a moderate QT prolongation without affecting TDR.

Prognostic Value of QT Interval, and Spatial and Transmural Dispersions

Amiodarone has differential effects of the two component delayed rectifier K^+ currents: rapidly component (I_{Kr}) and slowly component (I_{Ks}). Kamiya et al. reported that short-term treatment of amiodarone inhibited primarily I_{Kr}, whereas long-term treatment reduced I_{Ks} in the rabbit ventricular myocardium.[16] Lynch et al. suggested that selective blockade of I_{Ks} was useful to prevent ventricular arrhythmias even though the QTc interval was modestly (+7%) increased.[27] Recent studies suggested the excessive prolonged QTc interval was associated with the increase in mortality in patients with dofetilide treatment,[28] and advanced heart failure.[29] These previous studies have supported our data that patients without prolonged max QTce (< 510 ms) after chronic amiodarone had less recurrence of VT/VF compared to those with the excessive prolonged max QTce (≥510 ms).

On the other hand, several studies have investigated the value of QT dispersion in the 12-lead ECG for predicting ventricular arrhythmias or other adverse events in various cardiac diseases,[5,6] but the results are controversial.[30,31] Previous retrospective studies suggested no significant relationship between QT dispersion in the 12-lead ECG and further arrhythmic events after amiodarone.[20,21] Our results also showed no significant correlation between the repolarization parameters from the 12-lead ECG and further arrhythmic events after amiodarone. Although the variability of data in max QTce from the 12-lead ECG were not so different from that of the